ORIGINAL ARTICLE

CXCR3-expressing myeloid cells recruited to the hypothalamus protect against diet-induced body mass gain and metabolic dysfunction

Natalia F. Mendes[1,2], Ariane M. Zanesco[2], Cristhiane F. Aguiar[3], Gabriela F. Rodrigues-Luiz[4], Dayana C. da Silva[2], Jonathan F. Campos[2], Niels O. S. Câmara[5], Pedro M. M. de Moraes-Vieira[3], Eliana P. de Araújo[2,6,#], Licio A. Velloso[2,7,*,#]

[1]School of Medical Sciences, Department of Translational Medicine (Section of Pharmacology), University of Campinas, Brazil.
[2]Laboratory of Cell Signaling, Obesity and Comorbidities Research Center, University of Campinas, Brazil.
[3]Laboratory of Immunometabolism, Institute of Biology - University of Campinas, Brazil.
[4] Department of Microbiology, Immunology and Parasitology, Federal University of Santa Catarina, Brazil.
[5]Laboratory for Transplantation Immunobiology, Institute of Biomedical Sciences, University of Sao Paulo, Brazil.
[6]Faculty of Nursing, University of Campinas, Brazil.
[7]National Institute of Science and Technology on Neuroimmunomodulation, Rio de Janeiro, Brazil.

* Corresponding Authors:
Licio A. Velloso. Electronic address: lavellos@unicamp.br
Natalia F. Mendes. Eletronic address: natalia.mendesss@gmail.com
Laboratory of Cell Signaling-Obesity and Comorbidities Research Center, University of Campinas, 13083-864 Campinas, Brazil

# EPA and LAV contributed equally as supervisors of this study

Abstract

Microgliosis is an important component of diet-induced hypothalamic inflammation in obesity. A few hours after the introduction of a high-fat diet, the mediobasal hypothalamus resident microglia undergo morphological and functional changes toward an inflammatory phenotype. If the consumption of large amounts of dietary fats persists for long periods, bone marrow-derived myeloid cells are recruited and integrated into a new landscape of hypothalamic microglia. However, it is currently unknown what are the transcriptional signatures and specific functions exerted by either resident or recruited subsets of hypothalamic microglia. Here, the elucidation of the transcriptional signatures revealed that resident microglia undergo only minor changes in response to dietary fats; however, under the consumption of a high-fat diet, there are major transcriptional differences between resident and recruited microglia with a major impact on chemotaxis. In addition, in recruited microglia, there are major transcriptional differences between females and males with an important impact on transcripts involved in neurodegeneration and thermogenesis. The chemokine receptor CXCR3 emerged as one of the components of chemotaxis with the greatest difference between recruited and resident microglia, and thus, was elected for further intervention. The hypothalamic immunoneutralization of CXCL10, one of the ligands for CXCR3, resulted in increased body mass gain and reduced energy expenditure, particularly in females. Furthermore, the chemical inhibition of CXCR3 resulted in a much greater change in phenotype with increased body mass gain, reduced energy expenditure, increased blood leptin, glucose intolerance, and reduced insulin. Thus, this study has elucidated the transcriptional differences between resident and recruited hypothalamic microglia in diet-induced obesity, identifying chemokines as a relevant subset of genes undergoing regulation. In addition, we showed that a subset of recruited microglia expressing CXCR3 has a protective, rather than a detrimental role in the metabolic outcomes promoted by the consumption of a high-fat diet, thus, establishing a new concept in obesity-associated hypothalamic inflammation.

Keywords: Hypothalamus, obesity, monocytes, microglia, chemokines.

Introduction

Obesity affects over 600 million people worldwide and projections are pessimistic indicating that over a billion people will be diagnosed with obesity by the year 2030 (worldobesity.org). Obesity develops as a consequence of a chronic state of anabolism in which caloric intake overcomes energy expenditure [1]. Both, experimental and human studies have indicated that, at least in part, the chronic anabolic state leading to obesity develops as a consequence of a defective hypothalamic regulation of whole-body energy balance [2] [3] [4].

Experimental studies have shown that the consumption of large amounts of saturated fats triggers an inflammatory response in the hypothalamus affecting the function of key neurons involved in the regulation of food intake, energy expenditure, and systemic metabolism [5] [6] [7] [8]. In addition, human studies using magnetic resonance imaging have identified hypothalamic gliosis in adults and children with obesity, providing clinical evidence for the existence of an obesity-associated hypothalamic inflammation [4] [9] [10]. Microglia are key cellular components of this inflammatory response undergoing structural and functional changes that develop early after the introduction of a high-fat diet (HFD) [11] [12] [13] [14]. Distinct strategies used to inhibit hypothalamic microglia resulted in impaired diet-induced hypothalamic inflammation, increased leptin sensitivity, reduced spontaneous caloric intake, and improved systemic glucose tolerance [12] [15]. Thus, elucidating the mechanisms involved in the regulation of microglial response to dietary factors may provide an advance in the definition of the pathophysiology of obesity, and potentially identify new targets for interventions aimed at treating obesity and its metabolic comorbidities [16] [17] [18].

Resident microglia are derived from the yolk sac primitive hematopoietic cells and populate the neuroepithelium at embryonic day 9.5 [19]. Under baseline conditions, in the absence of infections, trauma, or other types of potentially harmful stimuli, resident microglia remain rather quiescent; however, under stimulus, they undergo rapid morphological and functional changes aimed at confronting the threat [20]. In the hypothalamus, differently from most parts of the brain, resident microglia are responsive to fluctuations in the blood levels of nutrients and hormones involved in metabolic control, such as leptin [12]. Thus, a simple meal can promote considerable changes in hypothalamic resident microglia indicating the involvement of these cells in the complex network of cells that regulate whole body metabolism [21]. Under the consumption of a nutritionally balanced diet, meal-induced changes in hypothalamic resident microglia are cyclic and completely reversible [21]. However, under consumption of an HFD, microglia present profound changes in morphology and function; moreover, upon prolonged consumption of this type of diet, there is recruitment of bone marrow-derived myeloid cells that will compose a new landscape of hypothalamic microglia [12] [15] [18]. Despite the considerable advance in the understanding of how hypothalamic microglia are involved in diet-induced obesity (DIO), the transcriptional landscapes of resident and recruited microglia are currently unknown; and, the specific functions of either subset of microglia remain elusive.

In this study, we first elucidated the transcriptional differences between resident and recruited hypothalamic microglia in DIO, identifying chemokines as a relevant subset of genes undergoing regulation. Next, we identified a subset of recruited microglia expressing CXCR3, which exerts a protective role against DIO.

Results

Elucidating the transcriptional signatures of hypothalamic resident and recruited microglia in diet-induced obesity. Double reporter mice were obtained by the crossing of $CX3CR1^{GFP}$ and $CCR2^{RFP}$ (Fig. 1a). At the age of 8 weeks, female and male mice were randomly selected for either chow or HFD feeding for 28 days, and then specimens were harvested for analysis (Fig. 1b). In flow cytometry, cells expressing CCR2 could not be detected in the hypothalamus of mice fed on chow (Fig. 1c), whereas in the white adipose tissue, virtually all cells expressing CX3CR1 were also expressing CCR2 (Fig. 1c). Conversely, in both female and male mice fed on HFD, CCR2 cells accounted for approximately 10% of hypothalamic microglia (Fig. 1d). Histological analysis confirmed the results obtained by flow cytometry (Fig. 1e); furthermore, it was shown that CD169, which is classically regarded as a marker of bone marrow-derived cells [22], is expressed both in resident as well as in recruited microglia (Fig. 1f), confirming data published elsewhere [18]. Next, to prepare the samples for RNA sequencing, we sorted hypothalamic microglia expressing either CX3CR1 or CCR2 (Fig. 2a). The quality of sorting was confirmed by determining positivity for CX3CR1 (Fig. 2b) and CCR2 (Fig. 2c), and also by determining the positivity for several markers of resident microglia (Fig. 2d-2m) and several markers of bone marrow-derived cells (Fig. 2n-2x). The elucidation of the transcriptional landscapes of CX3CR1 and CCR2 revealed that either diet or sex exerted only minor differences in the expression of transcripts in CX3CR1 cells (Fig. 3a-3b); nevertheless, sex exerted major differences in CCR2 cells (Fig. 3a-3b). The direct comparisons between CX3CR1 and CCR2 obtained from mice fed on the HFD revealed the vast differences in the transcriptional landscapes of either female (Fig. 3c) or male (Fig. 3d) mice. Furthermore, the direct comparisons between female and male mice revealed a considerable degree of sexual dimorphism in the transcriptional landscapes of recruited CCR2 cells (Fig. 3e). In CX3CR1 cells, the consumption of the HFD impacted on IL17, lipids, toll-like receptor signaling, tumor necrosis factor signaling and chemokines (Fig. 4a); whereas in CCR2 cells, the consumption of the HFD impacted on lipids, toll-like receptor signaling, tumor necrosis factor signaling, chemokines, neurotrophins signaling, reactive oxygen species, thermogenesis, and pathways related to neurodegeneration (Fig. 4a). Next, we asked what functions related to chemotaxis were predominantly regulated in CCR2 cells of mice fed on the HFD (Fig. 4b-4c). As cell chemotaxis emerged as an important function in both females (Fig. 4b) and males (Fig. 4c), we looked with greater detail into the expression of chemokines and chemokine receptors (Fig. 4d). Virtually all the transcripts evaluated showed diametrically opposite expression between CX3CR1 and CCR2 (Fig. 4d).

Cxcr3 is highly expressed in recruited microglia. As we were particularly interested in identifying factors involved in the recruitment of CCR2 to the hypothalamus, we evaluated cytokine receptors with high expression in CCR2 and low expression in CX3CR1. As depicted in Fig. 5, Ccr3 (Fig. 5a), Ccr7 (Fig. 5b), Ccr8 (Fig. 5c), Cxcr2 (Fig. 5d), Cxcr3 (Fig. 5e), Cxcr4 (Fig. 5f), Cxcr5 (Fig. 5g), Cxcr6 (Fig. 5h) and Cxcr7 (Fig. 5i) were all expressed in CCR2 cells and virtually absent from CX3CR1 cells. Cxcr3 (Fig. 5e) and Cxcr6 (Fig. 5h) presented the highest expressions, and therefore, we performed a search for previous studies looking at either of these chemokine receptors in the context of DIO hypothalamic inflammation. Using the terms, hypothalamus, hypothalamic, obesity, inflammation, Cxcr3, and Cxcr6, we could find no prior publications. As Cxcr3 is involved in interferon-gamma (IFN-γ) induction [23], and IFN-γ is expressed in the context of DIO hypothalamic inflammation [5], we looked into the IFN-γ-related pathways regulated in recruited microglia (Fig. 6). First, we asked if the canonical ligands for CXCR3, C*XCL9*, CCL10, and CXCL11, were expressed in either CX3CR1 or CCR2 cells. C*XCL11* was not

158 detected in either cell type (not shown). CXCL9 (Fig. 6a) was expressed in CX3CR1 cells, only,
159 whereas CXCL10 (Fig. 6b) was expressed in both CX3CR1 and CCR2 cells. In addition, in both
160 female and male mice, Ifng was expressed in CCR2, but not in CX3CR1 cells (Fig. 6c).
161 Furthermore, IFN-γ pathways were shown to be modulated in both female (Fig. 6d) and male
162 (Fig. 6e) CCR2 cells. Thus, we elected CXCR3 as a target for further intervention.

163 *The immunoneutralization of hypothalamic CXCL10 leads to increased body mass gain in*
164 *female mice.* As an attempt to interfere with CXCR3 actions in CCR2 cells, we targeted one of its
165 ligands, CXCL10. As depicted in Fig. 7a, mice were submitted to two intracerebroventricular
166 (icv) injections of an anti-CXCL10 antibody aimed at immunoneutralizing the target protein in
167 the hypothalamus. As a result of the immunoneutralization of CXCL10, there were smaller
168 numbers of CCR2-positive cells in the hypothalamus of both female and male mice fed on an
169 HFD (Fig. 7b). However, there were no major changes in the numbers of CXCR3-expressing cells
170 in the hypothalamus of either female (Fig. 7c) or male (Fig. 7d) mice fed on an HFD. This was
171 accompanied by no changes in the transcript levels of Cxcr3 and several other chemokine-
172 related transcripts (Fig. 7c-7d), except for a trend to decrease Cxcl11 and an increase of Cxcr4
173 in females (Fig. 7c); and a decrease of Cxcl10 and a trend to increase Cx3cl1 in males (Fig. 7d).
174 Nevertheless, the immunoneutralization of hypothalamic CXCL10 (Fig. 8 and Fig. 9) resulted in
175 increased body mass gain (Fig. 8a-8b), a trend to reduce blood triglycerides (Fig. 8f), reduced
176 blood cholesterol (Fig. 8g), reduced expression of Agrp transcript in the hypothalamus (Fig. 8k),
177 a trend to reduce blood insulin (Fig. 8n), trends to reduce Il1b and Il6 transcripts in the
178 hypothalamus (Fig. 8o), and a trend to reduce respiratory quotient (Fig. 8s) during the dark
179 cycle in female mice. Conversely, in male mice (Fig. 9), the inhibition of hypothalamic CXCL10
180 had only a minor effect, leading to a trend to reduce hypothalamic Npy (Fig. 9k), a trend to
181 reduce hypothalamic Il1b, and a trend to increase hypothalamic Il6 (Fig. 9o).

182 *The inhibition of CXCR3 worsens body mass gain and the metabolic phenotype of mice fed on a*
183 *high-fat diet.* CXCR3 was inhibited using a pharmacological antagonist, AMG487 [24] (Fig. 10a).
184 The intervention resulted in the reduction of CCR2 (Fig. 10b) and CXCR3 (Fig. 10c-10d) cells in
185 the hypothalamus of both female and male mice fed an HFD. In addition, there was a reduction
186 of Ccl2 and an increase of Cx3cl1 transcripts in the hypothalamus of females (Fig. 10e), and a
187 reduction of Ccl2 transcripts in the hypothalamus of male (Fig. 10f) mice fed an HFD. The
188 inhibition of CXCR3 had a major impact on metabolic phenotype; thus, in female mice fed an
189 HFD, there was an increase in body mass gain (Fig. 11a-11b), a trend to increase brown adipose
190 tissue mass (Fig. 11c), a trend to increase blood leptin (Fig. 11e), an increase in blood
191 triglycerides (Fig. 11f), a trend to reduce hypothalamic Pomc (Fig. 11k), an increase in
192 hypothalamic Npy (Fig. 11k), a worsen glucose tolerance (Fig. 11l), increased fasting blood
193 glucose (Fig. 11m), reduced blood insulin (Fig. 11n), and reduction of Il6 and Tlr4 transcripts in
194 the hypothalamus (Fig. 11o). In males, the inhibition of CXCR3 promoted an increased body
195 mass gain (Fig. 12a-12b), increased white adipose tissue mass (Fig. 12d), increased blood leptin
196 (Fig. 12e), increased hypothalamic Npy and Mch (Fig. 12k), and reduced hypothalamic Tnfa and
197 Nlrp3 (Fig. 12o).

198

199 **Discussion**

200 In this study, we elucidated the transcriptional landscapes of resident and recruited microglia in
201 the hypothalamus of mice. We showed that resident microglia undergo minor transcriptional
202 changes when mice are fed an HFD; however, there are vast differences when confronting

resident versus recruited microglia transcriptomes. Moreover, there is a considerable degree of sexual dimorphism in the transcriptomes of recruited microglia in mice fed an HFD. Upon exploration of the differences between resident and recruited microglia, we identified the chemokine receptor Cxcr3 as an interesting candidate for intervention as it was highly expressed in recruited cells. The inhibition of CXCR3 resulted in increased body mass gain, worsening of glucose intolerance, and increased expression of hypothalamic Npy. Thus, the study is the first to identify a subset of recruited microglia that has a protective role against the deleterious outcomes of DIO, therefore establishing a new concept in obesity-associated hypothalamic inflammation.

Early studies in this field have shown that dietary fats, particularly long-chain saturated fatty acids, trigger an inflammatory response in the MBH that emerges a few hours after the introduction of an HFD and progresses to chronicity if the consumption of the HFD persists for long [5] [6] [7]. Microglia play an important role in this inflammatory response, and studies have shown that during a prolonged consumption of an HFD, there is recruitment of bone marrow-derived cells to compose a new hypothalamic microglia landscape [9] [15] [18]. However, it was previously unknown what are the transcriptional signatures of hypothalamic resident and recruited microglia in DIO.

To elucidate the transcriptional landscapes of resident and recruited microglia, we initially prepared a double reporter mouse for CX3CR1 and CCR2. CX3CR1 encodes for fractalkine receptor and is highly expressed in resident microglia [25]. The creation of CX3CR1 reporter mice was regarded as an important step toward the characterization of resident microglia, and several studies in the field employ this model [26] [27]. Conversely, CCR2 is expressed only in bone marrow-derived cells and is regarded as a good marker for studying recruited microglia [25] [28]. The quality of our model was proven good as makers of resident microglia were present in CX3CR1 cells, only, whereas markers of recruited microglia were present in CCCR2 cells, only. Moreover, as previously described, we could find no CCR2 cells in the hypothalamus of mice fed chow [14] [18].

The first important, and previously unknown finding emerged from the comparison of the transcriptomes of resident microglia in mice fed chow versus mice fed an HFD. In females, there were only 34 transcripts undergoing significant changes between the two dietary conditions, whereas in males, the number was greater, 412, but still quite small considering the whole transcriptome of resident microglia [29]. In a study evaluating the single-cell transcriptomics of hypothalamic cells, the consumption of an HFD resulted in minor changes in the so-called macrophage-like cells [30]; however, the detailed transcriptional landscape of these cells was not explored in depth, so it is uncertain if it contained both resident and recruited microglia. In an experimental model of Alzheimer´s disease, which evaluated male and female mice, there were hippocampal resident microglial transcriptional changes of the same magnitude as the one we found in the hypothalamus, affecting approximately 300 genes [31]. In an experimental model of cerebral hemorrhage evaluating only males, the impact on microglia transcriptome was also small, affecting only 10% of the evaluated genes [32]. In addition, in a study evaluating transcriptional changes of resident microglia during aging [33], there were also important differences between female and male mice; and, the magnitude of the transcriptional changes occurring during aging was about the same as we see in the dietary intervention. Thus, it seems that in different brain regions and under distinct interventions, the magnitude of resident microglia transcriptional changes is quite small; however, the number of studies evaluating this question is not expressive; thus, further studies are needed to provide a

definitive view regarding the actual magnitude of plasticity of resident microglia. Despite the small number of transcripts undergoing changes in our model, the greatest impact occurred in the expression of genes related to IL-17 signaling, lipid metabolism, TLR signaling, TNF signaling, and chemokine signaling, which strongly supports the role of dietary lipids in the induction of an inflammatory response by the resident microglia, supporting previous studies in the field [6] [9] [15] [18]. Interestingly, IL17 signaling emerged as a major pathway modulated by DIO. In a recent study, we have shown that IL17 can act upon POMC neurons promoting a reduction in calorie intake [34]. The current finding of a transcriptional modulation of IL17-related genes in resident microglia opens a new perspective in the understanding of how inflammatory signals modulate the function of the hypothalamus in obesity, which should be explored in the future.

Next, we confronted the transcriptomes of resident and recruited microglia, and in this case, there were huge differences, reaching over 7,000 transcripts. Per se, this finding reveals a striking difference between resident and recruited microglia in the hypothalamus of mice fed an HFD. Nevertheless, despite this is new information regarding the hypothalamus, similar findings were reported in other brain regions submitted to distinct interventions, such as in an experimental model of glioma [35], in flavivirus infection [36], and in COVID-19 [37]. The evaluation of the main pathways differently expressed in the two cell subsets revealed major differences in lipids, toll-like receptor signaling, tumor necrosis factor signaling, chemokines, neurotrophins signaling, reactive oxygen species, thermogenesis, and pathways related to neurodegeneration. The impact of the consumption of an HFD on the regulation of lipid-related pathways, toll-like receptor, and tumor necrosis factor signaling has been widely explored in several previous studies, and interventions in these systems are known to mitigate the harmful effects of the diet [6] [9] [15] [18]. However, little has been done about the characterization of the mechanisms of chemotaxis that drive the recruitment of bone marrow-derived cells to the hypothalamus. Therefore, we looked with greater detail into the main chemokines and chemokine receptors differentially expressed in the two subsets of cells. We elected Cxcr3 because it was highly expressed in Ccr2 cells and presented low expression in Cx3cr1 cells. CXCR3 is a chemokine receptor that is involved in the recruitment of distinct types of bone marrow-derived monocytic cells, such as plasmacytoid monocytes [38], synovial tissue monocytes [39], and dendritic cells [40]. In the brain, CXCR3-expressing cells have been implicated in Alzheimer's disease and other age-dependent cognitive dysfunctions [41] [42], multiple sclerosis [43], epilepsy [44], and stoke [45]. However, no previous study has evaluated CXCR3 in the hypothalamus in the context of obesity.

First, we asked if the known ligands for CXCR3, and Infg, which is induced in response to the activation of CXCR3, were present in either subset of cells. We found Cxcl11 in neither cell subset; Cxcl9 was expressed in Cx3cl1 cells, only; Cxcl10 was expressed in both subsets of cells, with greater expression in Ccr2 cells; and Infg was expressed in Ccr2 cells only. Moreover, there was a considerable engagement of INF-γ-related pathways in Ccr2 cells of both female and male mice fed an HFD. Thus, we considered CXCR3 as a promising target for intervention.

Next, we intervened in one of the ligands for CXCR3, CXCL10. For that, we performed icv injections of an immunoneutralizing antibody, which resulted in smaller numbers of CCR2 cells in the hypothalamus. However, the intervention promoted minimal changes in the hypothalamic expression of transcripts encoding several components of the chemotaxis machinery. Nevertheless, in females, the inhibition of CXCL10 resulted in increased body mass gain, reduction of hypothalamic Agrp, trends to reduce hypothalamic Il1b and Il6, and a trend

to reduce blood insulin. In males, the phenotype was much milder, leading to minimal changes in hypothalamic Npy, Il1b, and Il6. Little is known about the involvement of CXCL10 in hypothalamic physiology and pathology. In a model of caloric restriction, there was an increase in the hypothalamic expression of Cxcl10 [46], and this was regarded as a component of the mechanism of neuroprotection induced by caloric restriction. In addition, in a model of hypothalamic inflammation elicited by exogenous LPS, Cxcl10 emerged as one of the transcripts undergoing the greatest increase in the hypothalamic paraventricular nucleus [47].

As CXCR3 can be engaged by distinct chemokines, we decided to use a broader intervention, pharmacologically inhibiting CXCR3. AMG487 is a chemical inhibitor of CXCR3 with an IC_{50} value of 8.0 nM [48]. Upon treatment with AMG487, there was a reduction of the migration of Ccr2 cells to the hypothalamus, which was accompanied by minimal changes in the expressions of chemokines and chemokine receptors. Under inhibition of CXCR3, both female and male mice presented increased body mass gain, which was accompanied by increased blood leptin, increased fasting glucose, increased hypothalamic Npy, and a reduction in markers of hypothalamic inflammation. There were no changes in caloric intake, however, there were reductions in energy expenditure during some periods during the 24 hours of recording.

These findings reveal that at least one subset of recruited microglia, have a protective rather than a harmful role in DIO-associated hypothalamic inflammation. This is a completely new concept in the field because all previous studies evaluating hypothalamic microglia in DIO reported that, once active in response to dietary fats, either resident or recruited microglia exerted inflammatory actions that impacted negatively energy balance and glucose tolerance [11] [12] [13] [15]. This concept has been recently explored in depth in a study that used elegant models to either activate or inactivate microglia [14] and the results confirm that, whenever manipulating microglia using approaches that are not specific for a given subset of cells, the net result is worsening of the metabolic phenotype when microglia is activated and improvement of the metabolic phenotype when microglia is inactivated. Thus, we believe that the subset of recruited microglia herein identified plays a regulatory role in hypothalamic inflammation.

In conclusion, this study elucidated the transcriptional landscapes of resident and recruited hypothalamic microglia in DIO. In resident microglia, the consumption of an HFD resulted in small changes in transcript expression, whereas the confrontation of the transcriptional landscapes of resident versus recruited microglia revealed broad differences that encompass lipids, toll-like receptor signaling, tumor necrosis factor signaling, chemokines, neurotrophins signaling, reactive oxygen species, thermogenesis, and pathways related to neurodegeneration. In addition, the study revealed a considerable sexual dimorphism in the transcriptional landscape of both resident and recruited microglia. The study also identified a subset of recruited microglia, expressing the chemokine receptor Cxcr3 that has a protective role against the harmful metabolic effects of the HFD; thus, providing a new concept in DIO-associated hypothalamic inflammation.

Materials and methods

Animal care and diets. All animal care and experimental procedures were conducted in accordance with the guidelines of the Brazilian College for Animal Experimentation and approved by the Institutional Animal Care and Use Committee (CEUA 5497-1/2020 and 6210-

1/2023). Heterozygous CX3CR1$^{GFP/+}$CCR2$^{RFP/+}$ mice were generated by mating CX3CR1^{GFP} homozygous mice (JAX#005582) with CCR2^{RFP} homozygous mice (JAX#017586). Genotypes of these mice were identified by polymerase chain reaction (PCR). Mice were fed on a standard chow diet (Nuvilab; 3.76 kcal/g; 12.6% energy from protein, 77.7% energy from carbohydrate, and 9.58% energy from fat) or high-fat diet (HFD) (5.28 kcal/g; 12.88% energy from protein, 27.1% energy from carbohydrate, and 60% energy from fat) according to the experimental protocols. Food and water were available ad libitum throughout the experimental periods, except for the protocols that required fasting. The room temperature was controlled (22-24 °C), and a light-dark cycle was maintained on a 12-hour on-off cycle.

Flow cytometry. For the separation of CX3CR1^{GFP+} and CCR2^{RFP+} cells from the white adipose tissue of CX3CR1$^{GFP/+}$CCR2$^{RFP/+}$ mice we collected the retroperitoneal fat depot of one animal fed on a HFD for 4 weeks. It was minced and digested with type VIII collagenase (0.5 mg/mL, Sigma-Aldrich) in PBS for 20 min at 37°C with shaking. After digestion, the suspension was filtered using a 100 µm cell filter. For isolation of the same cells from the hypothalamus, samples of five CX3CR1$^{GFP/+}$CCR2$^{RFP/+}$ mice fed on an HFD for 4 weeks were pooled together and gently pressed through a cell strainer (100 µm). The cell solution was subjected to a Percoll gradient (70/40%) for monocyte purification. Samples were acquired on a BDFacs Symphony instrument (BD Biosciences, USA) and then analyzed using FlowJo software.

Cell sorting. For cell sorting of CX3CR1^{GFP+} and CCR2^{RFP+} cells from the hypothalamus, we employed CX3CR1^{GFP} mice fed on chow diet and CX3CR1$^{GFP/+}$CCR2$^{RFP/+}$ mice fed on HFD for 4 weeks. Harvested hypothalami of 20-30 male or 20-30 female mice were pooled together for each sample and gently pressed through a cell strainer (100 µm). The cell solution was subjected to a Percoll gradient (70/40%) for monocyte purification. The sorting was conducted on a BDFacs Melody instrument (BD Biosciences, USA).

RNA-sequencing (RNA-Seq) and analysis. Cell-sorted CX3CR1 GFP+ and CCR2 RFP+ cell samples from the hypothalamus were lysed for RNA extraction using the RNAqueous Micro kit (Invitrogen). RNA integrity was analyzed on a Bioanalyzer RNA Pico 6000 chip at the Core Facility for Scientific Research – University of São Paulo (CEFAP-USP). Low input RNA-Seq library preparation (Takara SMART-Seq v4) and sequencing by Illumina NovaSeq S2 PE150 Sequencing Lane (40M read pairs/sample avg) were performed by Maryland Genomics (Institute for Genome Sciences - IGS, University of Maryland School of Medicine – Baltimore, USA). Illumina sequencing adapters and low-quality reads were removed with Trimmomatic. Trimmed reads were aligned to the mouse reference genome (GRCm39) by STAR. Aligned reads were mapped to features using HTSeq, and differential expression analyses were performed using the DESeq2 package. Genes having less than 3 CPM were excluded prior to statistical analysis, and differentially expressed genes (DEGs) were selected using as cutoffs the adjusted p-value < 0.05. Heatmaps were performed using Pheatmap and a list of DEGs was passed to EnrichR and cluster Profiler for enrichment analyses.

CXCL10 immunoneutralization. For central neutralization of CXCL10, 8-wk CCR2^{RFP} male and female mice underwent a stereotaxic surgery for ICV injections of anti-CXCL10 Monoclonal Antibody (2 ul, Cat# MA5-23774, Thermo Fischer). The control groups were ICV injected with Mouse IgG2a Isotype Control (2 ul, Cat#02-6200, Thermo Fischer). Two distinct ICV injections were performed on Day 0 and Day 14, respectively, of the experimental protocol. For that, mice were anesthetized with ketamine (100 mg/kg) and xylazine (10 mg/kg) and submitted to stereotaxic surgery (Ultra Precise–model 963, Kopf). ICV coordinates were [antero-posterior/lateral/depth to bregma]: -0.46/-1.0/−2.3 mm. Immediately after the first surgery, at

Day 0, mice began to be fed on HFD for 4 weeks. From Day 0 to Day 28 food intake and body weight were evaluated weekly.

CXCR3 antagonism. For systemic blockage of CXCR3, 8-wk $CCR2^{RFP}$ male and female mice underwent a treatment with AMG487 (Tocris Bioscience, Bristol, UK), an active and selective CXC chemokine receptor 3 (CXCR3) antagonist. The in vivo formulation of AMG487 was prepared in 20% hydroxypropyl-β-cyclodextrin (Sigma, St. Louis, MO). A 50% hydroxypropyl-β-cyclodextrin (Sigma, St. Louis, MO) solution was prepared and AMG487 was added to this solution, it was incubated in a sonicating water bath for 2 hours with occasional vortexing. Next, distilled water was added to give the appropriate final concentration of AMG487 in 20% of hydroxypropyl-β-cyclodextrin. This solution at 20% served as the vehicle. Mice were treated with AMG487 or vehicle (VEH group) intraperitoneally at 5 mg/kg every 48h throughout four weeks. During this period, mice were fed on HFD, and food intake and body weight were evaluated weekly.

Glucose tolerance test. On the 24th day of CXCR3 blockage and CXCL10 neutralization experimental protocols, mice were fasted for 6 hours, and blood glucose was measured via tail bleed at baseline and 15, 30, 60, 90, and 120 min after an intraperitoneal injection of glucose (2.0 g/kg).

Indirect calorimetry. The oxygen consumption (VO_2), carbon dioxide production (VCO_2), energy expenditure, and respiratory quotient (RQ) were measured using an indirect open-circuit calorimeter (Oxylet M3 system; PanLab/Harvard Apparatus, MA, USA). Mice were allowed to adapt for 12 hours before data were recorded for 24 hours (light and dark cycles).

Immunofluorescence. On the day 28th of CXCR3 blockage and CXCL10 neutralization experimental protocols, male and female mice were perfused with 0,9% saline followed by 4% formaldehyde by cardiac canulation. Brains were extracted and incubated in 4% formaldehyde overnight at 4 °C for extended fixation. The brains were then incubated in 30% sucrose at 4 °C for 48h. A series of 20 µm-thick frozen sections (4 series equally) were prepared using a cryostat and stored in an anti-freezing solution. For the free-floating immunostaining, slices were washed with 0.1 M phosphate-buffered saline (PBS) (3 times, 5 min each) and blocked with 0.2% Triton X-100 and 5% donkey serum in 0.1 M PBS for 2 h at room temperature. Slices were incubated overnight at 4 °C with Anti-Cxcr3 (1:200, Cat# NB100-56404, Novus Biologicals) or Anti-Sialoadhesin/CD169 (1:200, ab18619, Abcam) in a blocking solution. After washing with 0.1 M phosphate-buffered saline (PBS) (3 times, 5 min each), sections were incubated with fluorophore-labeled secondary antibody (donkey anti-rabbit Alexa Fluor 405, 1:500, Cat# A48258, Invitrogen or goat anti-mouse Alexa Fluor 405, 1:500, Cat# A31553, Invitrogen) in a blocking solution for 2 h at room temperature. After washing again with 0.1 M phosphate-buffered saline (PBS) (3 times, 5 min each), brain slices were mounted onto slides with ProLong Diamond antifade mountant (Cat# P36930, Thermo Fischer). Sections were visualized with a Zeiss LSM780, confocal microscope (Carl Zeiss AG, Germany) at the National Institute of Photonics Applied to Cell Biology (INFABIC) at the University of Campinas.

Quantitative reverse transcription-polymerase chain reaction (qRT-PCR). Total RNA was extracted using a TRIzol reagent (Thermo Fisher Scientific) and synthesized cDNA with a High-Capacity cDNA Reverse Transcription Kit (HighCapacity cDNA Reverse Transcription Kit, Life Technologies). Real-time PCR reactions were run using the TaqMan system (Applied Biosystems). Primers used were Cxcr3 (Mm99999054_s1); Cxcl9 (Mm00434946_m1), Cxcl10 (Mm00445235_m1); Cxcl11 (Mm00444662_m1); Ccl2 (Mm00441242_m1); Cxcr4

(Mm01996749_s1); Cxcl12 (Mm00445553_m1), Cxcr6(Mm02620517_s1), Cxcl16 (Mm00469712_m1), Cx3cl1(Mm00436454_m1), Pomc (Mm00435874_m1), Agrp (Mm00475829_g1); Npy (Mm00445771_m1); Cartpt (Mm04210469_m1), Pmch (Mm01242886_g1), Tnfa (Mm00443258_m1), Il1b (Mm00434228_m1), Il6 (Mm00446190_m1), Nlrp3 (Mm00840904_m1), Tlr4 (Mm00445273_m1), Infg (Mm01168134_m1). GAPDH (Mm99999915_g1) was employed as a reference gene. Gene expression was obtained using the QuantStudio 6 (Thermo Fischer Scientific).

Hormonal and biochemical determinations. Serum insulin and leptin were measured by an enzyme-linked immunosorbent assay (ELISA) kit (#EZRMI-13K and #EZML-82K; Millipore). Serum triglyceride levels and total cholesterol were measured using a commercial colorimetric assay kit (LaborLab®, Guarulhos - SP, Brazil) following the manufacturer's instructions.

Statistical analysis. Data are presented as means ± standard error of the mean (SEM). The statistical analyses were carried out using a non-parametric Mann-Whitney test or two-way analysis of variance (ANOVA) when appropriate. Post hoc comparisons were performed using Sidak's test. Statistical significances were analyzed using Prism 8.0 software (GraphPad Software, La Jolla, CA). A p-value ≤0.05 was considered statistically significant.

Declaration of Interests/Relevant conflicts of interests/Financial disclosures. All authors declare no competing financial or other interests regarding this study.

Authors' contributions. NFM, EPA and LAV designed and planned the study; NFM, AMZ, DCS, and JFC performed most of the experiments; NFM and CFA performed FACS and cytometry analysis; GFL conducted bioinformatic analysis; NOSC provided animals models; PMMM-V supervised the work of CFA and provided equipment and methods for FACS and cytometry; NFM, EPA, and LAV discussed the data. NFM and LAV wrote the manuscript and prepared figures; EPA supervised NFM during her doctorate program. All authors read and approved the final manuscript.

Funding. This research was funded by The Sao Paulo Research Foundation (FAPESP): 2013/07607-8; 2017/22511-8; and 2021/00443-6.

Data Availability. Data will be available upon request to the corresponding author, L.A.V (lavellos@unicamp.br).

Acknowledgments. We are grateful to Erika Roman, Joseane Morari, Marcio Cruz, and Gerson Ferraz for laboratory management.

References

[1] Theilade, S., Christensen, M.B., Vilsbøll, T., Knop, F.K., 2021. An overview of obesity mechanisms in humans: Endocrine regulation of food intake, eating behaviour and common determinants of body weight. Diabetes, Obesity & Metabolism 23 Suppl 1: 17–35, Doi: 10.1111/dom.14270.

[2] Cavadas, C., Aveleira, C.A., Souza, G.F.P., Velloso, L.A., 2016. The pathophysiology of defective proteostasis in the hypothalamus - from obesity to ageing. Nature Reviews. Endocrinology 12(12): 723–33, Doi: 10.1038/nrendo.2016.107.

[3] Sonnefeld, L., Rohmann, N., Geisler, C., Laudes, M., 2023. Is human obesity an inflammatory disease of the hypothalamus? European Journal of Endocrinology 188(3): R37–45, Doi: 10.1093/ejendo/lvad030.

[4] van de Sande-Lee, S., Melhorn, S.J., Rachid, B., Rodovalho, S., De-Lima-Junior, J.C., Campos, B.M., et al., 2020. Radiologic evidence that hypothalamic gliosis is improved after bariatric surgery in obese women with type 2 diabetes. International Journal of Obesity (2005) 44(1): 178–85, Doi: 10.1038/s41366-019-0399-8.

[5] De Souza, C.T., Araujo, E.P., Bordin, S., Ashimine, R., Zollner, R.L., Boschero, A.C., et al., 2005. Consumption of a fat-rich diet activates a proinflammatory response and induces insulin resistance in the hypothalamus. Endocrinology 146(10): 4192–9, Doi: 10.1210/en.2004-1520.

[6] Milanski, M., Degasperi, G., Coope, A., Morari, J., Denis, R., Cintra, D.E., et al., 2009. Saturated fatty acids produce an inflammatory response predominantly through the activation of TLR4 signaling in hypothalamus: implications for the pathogenesis of obesity. The Journal of Neuroscience: The Official Journal of the Society for Neuroscience 29(2): 359–70, Doi: 10.1523/JNEUROSCI.2760-08.2009.

[7] Zhang, X., Zhang, G., Zhang, H., Karin, M., Bai, H., Cai, D., 2008. Hypothalamic IKKbeta/NF-kappaB and ER stress link overnutrition to energy imbalance and obesity. Cell 135(1): 61–73, Doi: 10.1016/j.cell.2008.07.043.

[8] Milanski, M., Arruda, A.P., Coope, A., Ignacio-Souza, L.M., Nunez, C.E., Roman, E.A., et al., 2012. Inhibition of hypothalamic inflammation reverses diet-induced insulin resistance in the liver. Diabetes 61(6): 1455–62, Doi: 10.2337/db11-0390.

[9] Thaler, J.P., Yi, C.-X., Schur, E.A., Guyenet, S.J., Hwang, B.H., Dietrich, M.O., et al., 2012. Obesity is associated with hypothalamic injury in rodents and humans. The Journal of Clinical Investigation 122(1): 153–62, Doi: 10.1172/JCI59660.

[10] Sewaybricker, L.E., Schur, E.A., Melhorn, S.J., Campos, B.M., Askren, M.K., Nogueira, G.A.S., et al., 2019. Initial evidence for hypothalamic gliosis in children with obesity by quantitative T2 MRI and implications for blood oxygen-level dependent response to glucose ingestion. Pediatric Obesity 14(2): e12486, Doi: 10.1111/ijpo.12486.

[11] Tapia-González, S., García-Segura, L.M., Tena-Sempere, M., Frago, L.M., Castellano, J.M., Fuente-Martín, E., et al., 2011. Activation of microglia in specific hypothalamic nuclei and the cerebellum of adult rats exposed to neonatal overnutrition. Journal of Neuroendocrinology 23(4): 365–70, Doi: 10.1111/j.1365-2826.2011.02113.x.

[12] Valdearcos, M., Robblee, M.M., Benjamin, D.I., Nomura, D.K., Xu, A.W., Koliwad, S.K., 2014. Microglia dictate the impact of saturated fat consumption on hypothalamic inflammation and neuronal function. Cell Reports 9(6): 2124–38, Doi: 10.1016/j.celrep.2014.11.018.

[13] Fernández-Arjona, M.D.M., León-Rodríguez, A., Grondona, J.M., López-Ávalos, M.D., 2022. Long-term priming of hypothalamic microglia is associated with energy balance disturbances under diet-induced obesity. Glia 70(9): 1734–61, Doi: 10.1002/glia.24217.

[14] Valdearcos, M., Douglass, J.D., Robblee, M.M., Dorfman, M.D., Stifler, D.R., Bennett, M.L., et al., 2017. Microglial Inflammatory Signaling Orchestrates the Hypothalamic Immune Response to Dietary Excess and Mediates Obesity Susceptibility. Cell Metabolism 26(1): 185-197.e3, Doi: 10.1016/j.cmet.2017.05.015.

[15] Morari, J., Anhe, G.F., Nascimento, L.F., de Moura, R.F., Razolli, D., Solon, C., et al., 2014. Fractalkine (CX3CL1) is involved in the early activation of hypothalamic inflammation in experimental obesity. Diabetes 63(11): 3770–84, Doi: 10.2337/db13-1495.

[16] Mendes, N.F., Kim, Y.-B., Velloso, L.A., Araújo, E.P., 2018. Hypothalamic Microglial Activation in Obesity: A Mini-Review. Frontiers in Neuroscience 12: 846, Doi: 10.3389/fnins.2018.00846.

[17] Mendes, N.F., Velloso, L.A., 2022. Perivascular macrophages in high-fat diet-induced hypothalamic inflammation. Journal of Neuroinflammation 19(1): 136, Doi: 10.1186/s12974-022-02519-6.

[18] Valdearcos, M., Myers, M.G., Koliwad, S.K., 2019. Hypothalamic microglia as potential regulators of metabolic physiology. Nature Metabolism 1(3): 314–20, Doi: 10.1038/s42255-019-0040-0.

[19] Ginhoux, F., Greter, M., Leboeuf, M., Nandi, S., See, P., Gokhan, S., et al., 2010. Fate Mapping Analysis Reveals That Adult Microglia Derive from Primitive Macrophages. Science 330(6005): 841–5, Doi: 10.1126/science.1194637.

[20] Saijo, K., Glass, C.K., 2011. Microglial cell origin and phenotypes in health and disease. Nature Reviews Immunology 11(11): 775–87, Doi: 10.1038/nri3086.

[21] Gao, Y., Ottaway, N., Schriever, S.C., Legutko, B., García-Cáceres, C., de la Fuente, E., et al., 2014. Hormones and diet, but not body weight, control hypothalamic microglial activity. Glia 62(1): 17–25, Doi: 10.1002/glia.22580.

[22] Chávez-Galán, L., Olleros, M.L., Vesin, D., Garcia, I., 2015. Much More than M1 and M2 Macrophages, There are also CD169(+) and TCR(+) Macrophages. Frontiers in Immunology 6: 263, Doi: 10.3389/fimmu.2015.00263.

[23] Cole, K.E., Strick, C.A., Paradis, T.J., Ogborne, K.T., Loetscher, M., Gladue, R.P., et al., 1998. Interferon-inducible T cell alpha chemoattractant (I-TAC): a novel non-ELR CXC chemokine with potent activity on activated T cells through selective high affinity binding to CXCR3. The Journal of Experimental Medicine 187(12): 2009–21, Doi: 10.1084/jem.187.12.2009.

[24] Walser, T.C., Rifat, S., Ma, X., Kundu, N., Ward, C., Goloubeva, O., et al., 2006. Antagonism of CXCR3 inhibits lung metastasis in a murine model of metastatic breast cancer. Cancer Research 66(15): 7701–7, Doi: 10.1158/0008-5472.CAN-06-0709.

[25] Greter, M., Lelios, I., Croxford, A.L., 2015. Microglia Versus Myeloid Cell Nomenclature during Brain Inflammation. Frontiers in Immunology 6, Doi: 10.3389/fimmu.2015.00249.

[26] Yona, S., Kim, K.-W., Wolf, Y., Mildner, A., Varol, D., Breker, M., et al., 2013. Fate Mapping Reveals Origins and Dynamics of Monocytes and Tissue Macrophages under Homeostasis. Immunity 38(1): 79–91, Doi: 10.1016/j.immuni.2012.12.001.

[27] Goldmann, T., Wieghofer, P., Müller, P.F., Wolf, Y., Varol, D., Yona, S., et al., 2013. A new type of microglia gene targeting shows TAK1 to be pivotal in CNS autoimmune inflammation. Nature Neuroscience 16(11): 1618–26, Doi: 10.1038/nn.3531.

[28] Mildner, A., Schmidt, H., Nitsche, M., Merkler, D., Hanisch, U.-K., Mack, M., et al., 2007. Microglia in the adult brain arise from Ly-6ChiCCR2+ monocytes only under defined host conditions. Nature Neuroscience 10(12): 1544–53, Doi: 10.1038/nn2015.

[29] Young, A.M.H., Kumasaka, N., Calvert, F., Hammond, T.R., Knights, A., Panousis, N., et al., 2021. A map of transcriptional heterogeneity and regulatory variation in human microglia. Nature Genetics 53(6): 861–8, Doi: 10.1038/s41588-021-00875-2.

[30] Campbell, J.N., Macosko, E.Z., Fenselau, H., Pers, T.H., Lyubetskaya, A., Tenen, D., et al., 2017. A molecular census of arcuate hypothalamus and median eminence cell types. Nature Neuroscience 20(3): 484–96, Doi: 10.1038/nn.4495.

[31] Rivera-Escalera, F., Pinney, J.J., Owlett, L., Ahmed, H., Thakar, J., Olschowka, J.A., et al., 2019. IL-1β-driven amyloid plaque clearance is associated with an expansion of transcriptionally reprogrammed microglia. Journal of Neuroinflammation 16(1): 261, Doi: 10.1186/s12974-019-1645-7.

[32] Taylor, R.A., Chang, C.-F., Goods, B.A., Hammond, M.D., Mac Grory, B., Ai, Y., et al., 2017. TGF-β1 modulates microglial phenotype and promotes recovery after intracerebral hemorrhage. The Journal of Clinical Investigation 127(1): 280–92, Doi: 10.1172/JCI88647.

[33] Li, X., Li, Y., Jin, Y., Zhang, Y., Wu, J., Xu, Z., et al., 2023. Transcriptional and epigenetic decoding of the microglial aging process. Nature Aging, Doi: 10.1038/s43587-023-00479-x.

[34] Nogueira, G., Solon, C., Carraro, R.S., Engel, D.F., Ramalho, A.F., Sidarta-Oliveira, D., et al., 2020. Interleukin-17 acts in the hypothalamus reducing food intake. Brain, Behavior, and Immunity 87: 272–85, Doi: 10.1016/j.bbi.2019.12.012.

[35] Ochocka, N., Segit, P., Walentynowicz, K.A., Wojnicki, K., Cyranowski, S., Swatler, J., et al., 2021. Single-cell RNA sequencing reveals functional heterogeneity of glioma-associated brain macrophages. Nature Communications 12(1): 1151, Doi: 10.1038/s41467-021-21407-w.

[36] Spiteri, A.G., Wishart, C.L., Ni, D., Viengkhou, B., Macia, L., Hofer, M.J., et al., 2023. Temporal tracking of microglial and monocyte single-cell transcriptomics in lethal flavivirus infection. Acta Neuropathologica Communications 11(1): 60, Doi: 10.1186/s40478-023-01547-4.

[37] Schwabenland, M., Salié, H., Tanevski, J., Killmer, S., Lago, M.S., Schlaak, A.E., et al., 2021. Deep spatial profiling of human COVID-19 brains reveals neuroinflammation with distinct microanatomical microglia-T-cell interactions. Immunity 54(7): 1594-1610.e11, Doi: 10.1016/j.immuni.2021.06.002.

[38] Cella, M., Jarrossay, D., Facchetti, F., Alebardi, O., Nakajima, H., Lanzavecchia, A., et al., 1999. Plasmacytoid monocytes migrate to inflamed lymph nodes and produce large amounts of type I interferon. Nature Medicine 5(8): 919–23, Doi: 10.1038/11360.

[39] Katschke, K.J., Rottman, J.B., Ruth, J.H., Qin, S., Wu, L., LaRosa, G., et al., 2001. Differential expression of chemokine receptors on peripheral blood, synovial fluid, and synovial tissue monocytes/macrophages in rheumatoid arthritis. Arthritis and Rheumatism 44(5): 1022–32, Doi: 10.1002/1529-0131(200105)44:5<1022::AID-ANR181>3.0.CO;2-N.

[40] Padovan, E., Spagnoli, G.C., Ferrantini, M., Heberer, M., 2002. IFN-alpha2a induces IP-10/CXCL10 and MIG/CXCL9 production in monocyte-derived dendritic cells and enhances their capacity to attract and stimulate CD8+ effector T cells. Journal of Leukocyte Biology 71(4): 669–76.

[41] Jorfi, M., Park, J., Hall, C.K., Lin, C.-C.J., Chen, M., von Maydell, D., et al., 2023. Infiltrating CD8+ T cells exacerbate Alzheimer's disease pathology in a 3D human neuroimmune axis model. Nature Neuroscience 26(9): 1489–504, Doi: 10.1038/s41593-023-01415-3.

[42] Schroer, A.B., Ventura, P.B., Sucharov, J., Misra, R., Chui, M.K.K., Bieri, G., et al., 2023. Platelet factors attenuate inflammation and rescue cognition in ageing. Nature 620(7976): 1071–9, Doi: 10.1038/s41586-023-06436-3.

[43] Bogers, L., Engelenburg, H.J., Janssen, M., Unger, P.-P.A., Melief, M.-J., Wierenga-Wolf, A.F., et al., 2023. Selective emergence of antibody-secreting cells in the multiple sclerosis brain. EBioMedicine 89: 104465, Doi: 10.1016/j.ebiom.2023.104465.

[44] Liang, P., Zhang, X., Zhang, Y., Wu, Y., Song, Y., Wang, X., et al., 2023. Neurotoxic A1 astrocytes promote neuronal ferroptosis via CXCL10/CXCR3 axis in epilepsy. Free Radical Biology & Medicine 195: 329–42, Doi: 10.1016/j.freeradbiomed.2023.01.002.

[45] Cai, W., Shi, L., Zhao, J., Xu, F., Dufort, C., Ye, Q., et al., 2022. Neuroprotection against ischemic stroke requires a specific class of early responder T cells in mice. The Journal of Clinical Investigation 132(15): e157678, Doi: 10.1172/JCI157678.

[46] Matthews, D., Diskin, M.G., Kenny, D.A., Creevey, C.J., Keogh, K., Waters, S.M., 2017. Effect of short term diet restriction on gene expression in the bovine hypothalamus using next generation RNA sequencing technology. BMC Genomics 18(1): 857, Doi: 10.1186/s12864-017-4265-6.

[47] Reyes, T.M., Walker, J.R., DeCino, C., Hogenesch, J.B., Sawchenko, P.E., 2003. Categorically distinct acute stressors elicit dissimilar transcriptional profiles in the paraventricular nucleus of the hypothalamus. The Journal of Neuroscience: The Official Journal of the Society for Neuroscience 23(13): 5607–16, Doi: 10.1523/JNEUROSCI.23-13-05607.2003.

[48] Johnson, M., Li, A.-R., Liu, J., Fu, Z., Zhu, L., Miao, S., et al., 2007. Discovery and optimization of a series of quinazolinone-derived antagonists of CXCR3. Bioorganic & Medicinal Chemistry Letters 17(12): 3339–43, Doi: 10.1016/j.bmcl.2007.03.106.

Table

Table 1. Number of DEGs for each comparison

		↑ Up	↓ Down
Effect of the diet in brain resident microglia cells	**hfd_cx_f** Cx3cr1_hfd_female *vs.* Cx3cr1_chow_female	25	9
	hfd_cx_m Cx3cr1_hfd_male *vs.* Cx3cr1_chow_male	261	151
Effect of the sex in brain resident microglia cells	**chow_cx** Cx3cr1_chow_male *vs.* Cx3cr1_chow_female	9	11
	hfd_cx Cx3cr1_hfd_male *vs.* Cx3cr1_hfd_female	7	5
Brain resident microglia cells *vs.* infiltrating cells	**hfd_cc_f** Cx3cr1_hfd_female *vs.* Ccr2_hfd_female	4036	3569
	hfd_cc_m Cx3cr1_hfd_male *vs.* Ccr2_hfd_male	3838	3350
Effect of the sex in infiltrating cells	**hfd_cc** Ccr2_hfd_male *vs.* Ccr2_hfd_female	1598	1676

627 **Figures**

628

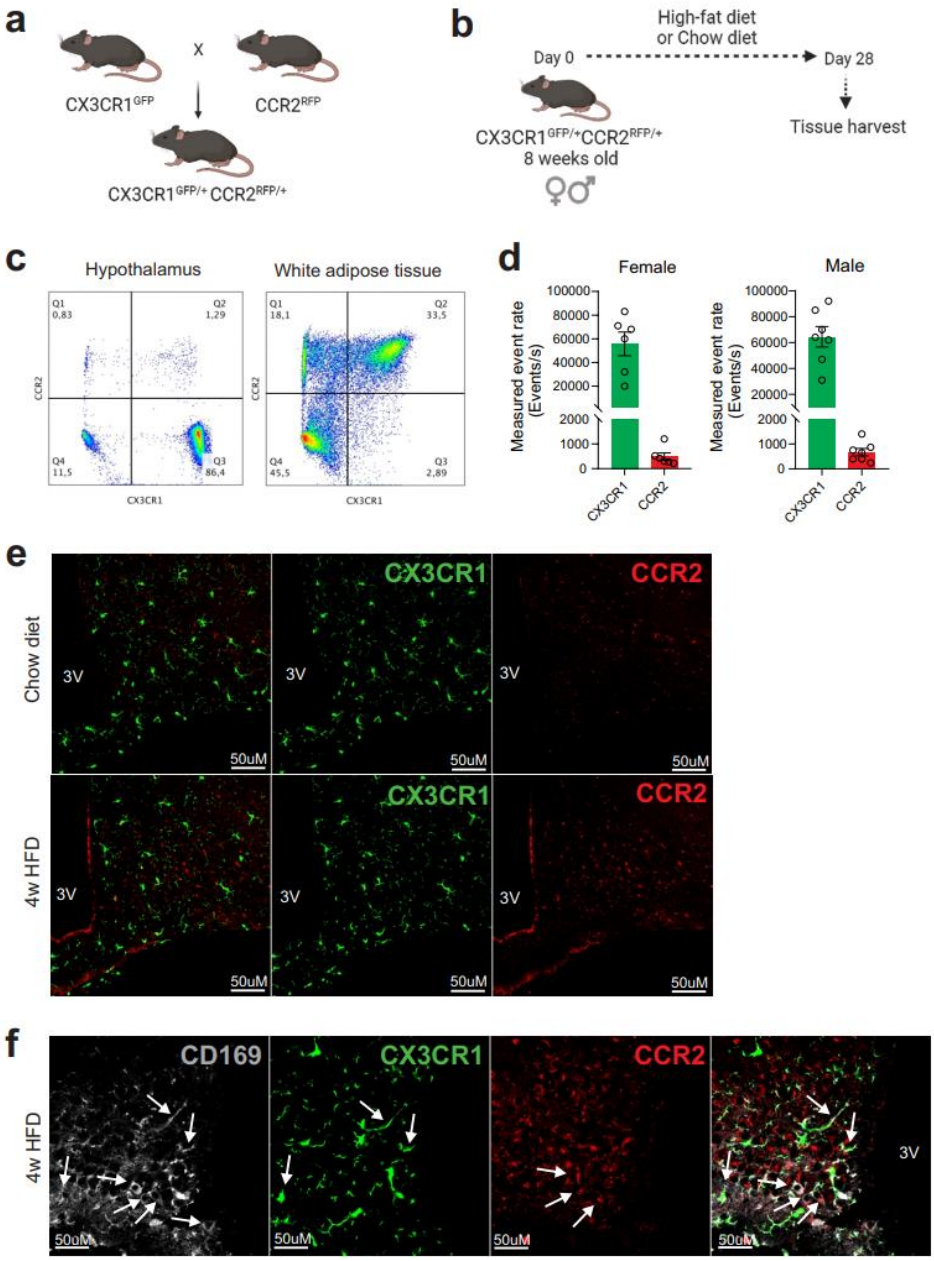

629

630 **Figure 1. CCR2+ cells infiltrate the hypothalamus of mice fed a high-fat diet.** a) CX3CR1$^{GFP/+}$CCR2$^{RFP/+}$
631 dual-reporter mutant mice generation. b) Schematic representation of the experimental protocol for
632 analysis of HFD-induced CCR2+ peripheral-cell chemotaxis towards the hypothalamus. c) Flow cytometry
633 analysis of CX3CR1^{GFP+} and CCR2^{RFP+} cells in the white adipose tissue and in the hypothalamus of HFD-fed
634 mice. d) Measured event rate detected by flow cytometer of CX3CR1^{GFP+} and CCR2^{RFP+} cells isolated from
635 the hypothalamus of HFD-fed male and female mice. e) Coronal brain sections of mediobasal
636 hypothalamus (MBH) from chow- and 4 weeks HFD-fed mice CX3CR1$^{GFP/+}$CCR2$^{RFP/+}$. f) Coronal brain
637 sections of MBH from 4 weeks HFD-fed mice CX3CR1$^{GFP/+}$CCR2$^{RFP/+}$ immunostained for CD169
638 (Sialoadhesin). White arrows indicate overlap between CD169+ cells with CX3CR1+ cells or with CCR2+
639 cells. 3V = Third ventricle, Scale Bar = 50 µm.

640

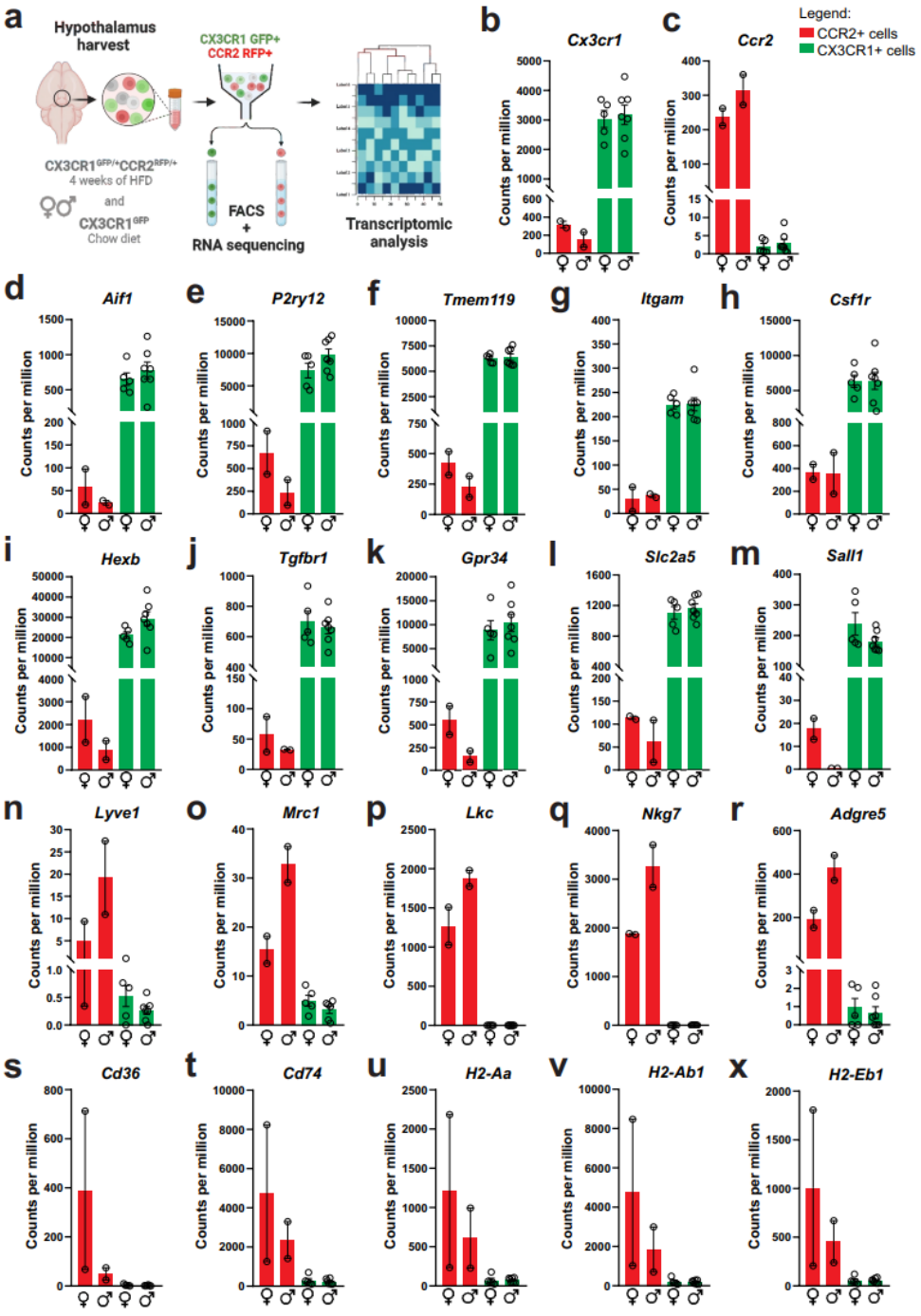

Figure 2. CX3CR1+ resident and CCR2+ recruited cells sorted from the hypothalamus of HFD-fed mice express classical markers of microglia and other immune cells. a) Schematic representation of the experimental protocol for sorting and sequencing CX3CR1+ and CCR2+ cells from the hypothalamus of chow- and HFD-fed mice. b) Cx3cr1 gene expression and c) Ccr2 gene expression of CX3CR1+ and CCR2+ cells sorted from the hypothalamus of HFD-fed mice. Analysis of d-m) classical microglial markers and n-x) bone marrow-derived immune cell markers in the transcriptome of CX3CR1+ and CCR2+ cells sorted from the hypothalamus of HFD-fed mice. To perform RNA-sequencing we have employed a total of 200 mice of each sex fed on HFD and 100 mice of each sex fed on chow diet. They were divided in 5 independent experiments. In order to get total RNA amount from CCR2+ cells in the hypothalamus of HFD-fed mice that was enough for library construction and RNA-seq, CCR2+ samples were pooled together in 3 samples, but only 2 samples could be sequenced due the final RNA integrity and amount.

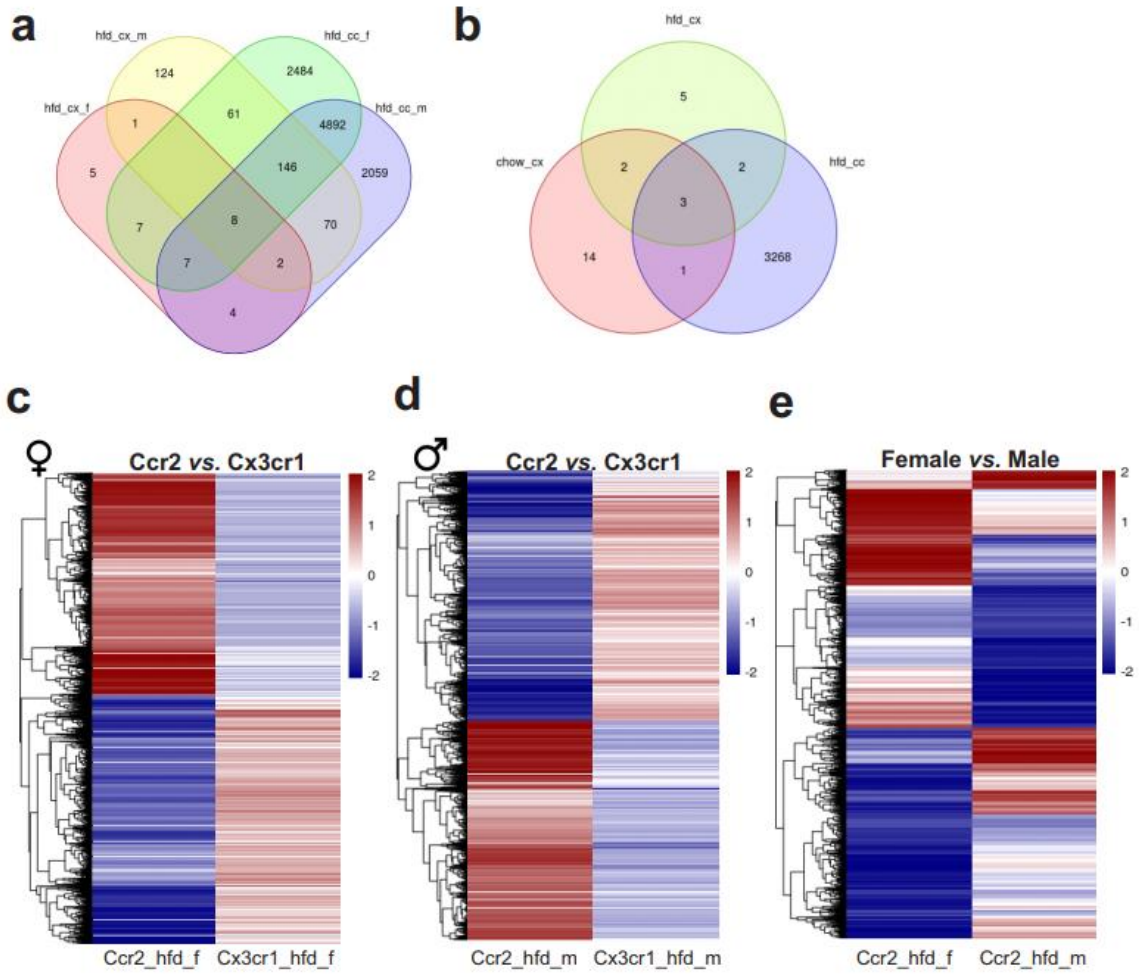

654

655 **Figure 3. Differential gene expression (DGE) analysis of CX3CR1+ resident microglia and CCR2+**
656 **infiltrating cells sorted from the hypothalamus of HFD-fed mice show an enormous difference in their**
657 **transcriptomic signature.** A-b) Venn diagram showing the number of DGEs for chow and HFD diet
658 comparison and sex comparison, respectively. c) Heatmap of up and downregulated DEGs when
659 comparing CX3CR1+ resident and CCR2+ infiltrating cells from HFD-fed female mice. d) Heatmap of up
660 and downregulated DEGs when comparing CX3CR1+ resident and CCR2+ infiltrating cells from HFD-fed
661 male mice. e) Heatmap of up and downregulated DEGs when comparing CCR2+ infiltrating cells from
662 HFD-fed male and female mice. hfd_cx_f = Cx3cr1_hfd_female vs. Cx3cr1_chow_female; hfd_cx_m =
663 Cx3cr1_hfd_male vs. Cx3cr1_chow_male; chow_cx = Cx3cr1_chow_male vs. Cx3cr1_chow_female;
664 hfd_cx = Cx3cr1_hfd_male vs. Cx3cr1_hfd_female; hfd_cc_f = Cx3cr1_hfd_female vs. Ccr2_hfd_female;
665 hfd_cc_m = Cx3cr1_hfd_male vs. Ccr2_hfd_male; hfd_cc = Ccr2_hfd_male vs. Ccr2_hfd_female.

666

667

668

669

670

671

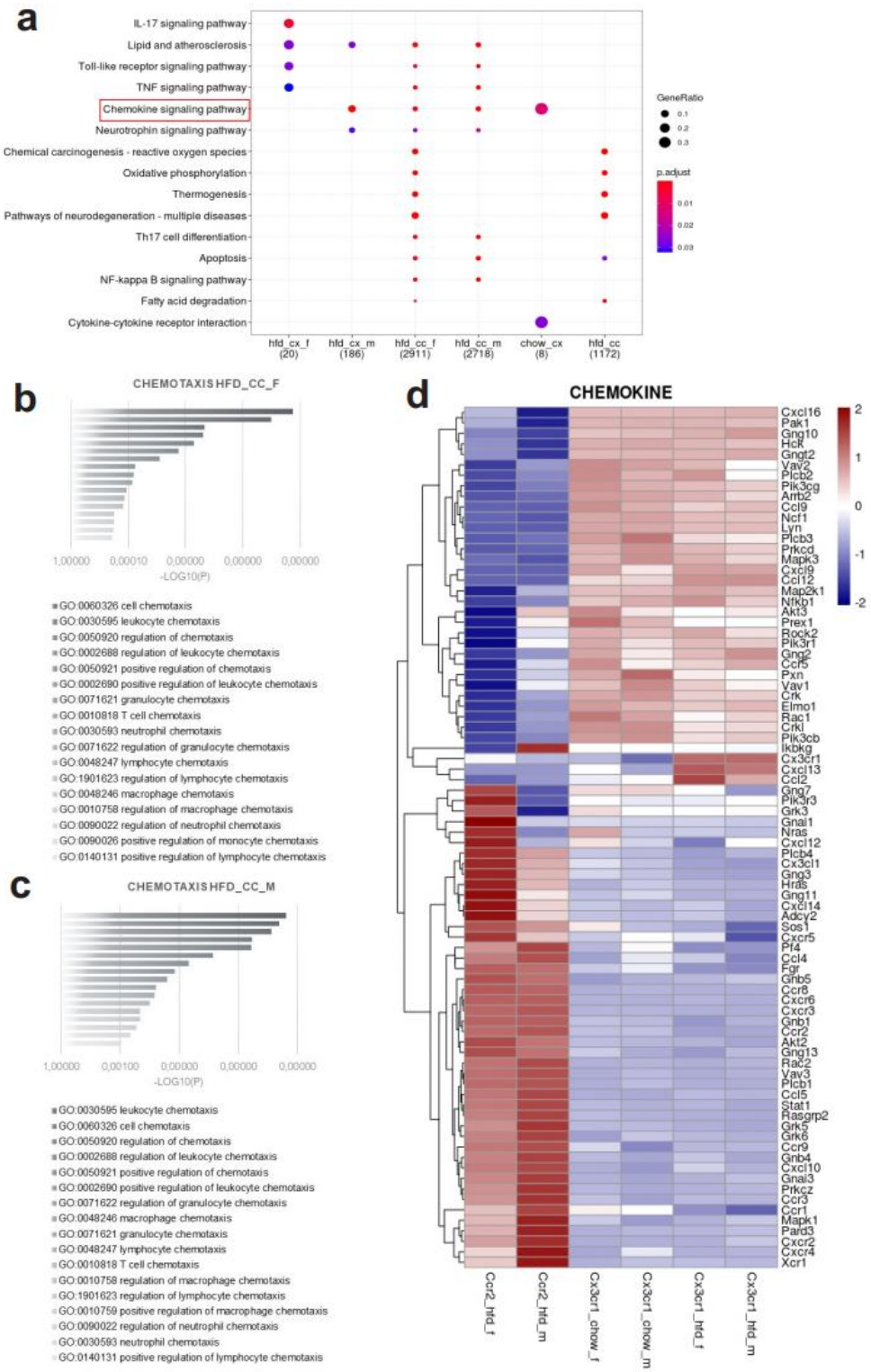

Figure 4. Various differential gene expression (DGE) found in CCR2+ infiltrating cells from hypothalamus of HFD-fed mice belongs to chemotaxis pathways. a) KEGG enrichment analysis shows the distribution of DGEs in distinct metabolic pathways. b-c) Ontology analysis for DGEs related to chemotaxis from CCR2+ cells sorted from the hypothalamus of HFD-fed female and male mice, respectively. d) Heatmap of up and downregulated DEGs related to chemotaxis when comparing CX3CR1+ resident and CCR2+ infiltrating cells from HFD-fed male and female mice.

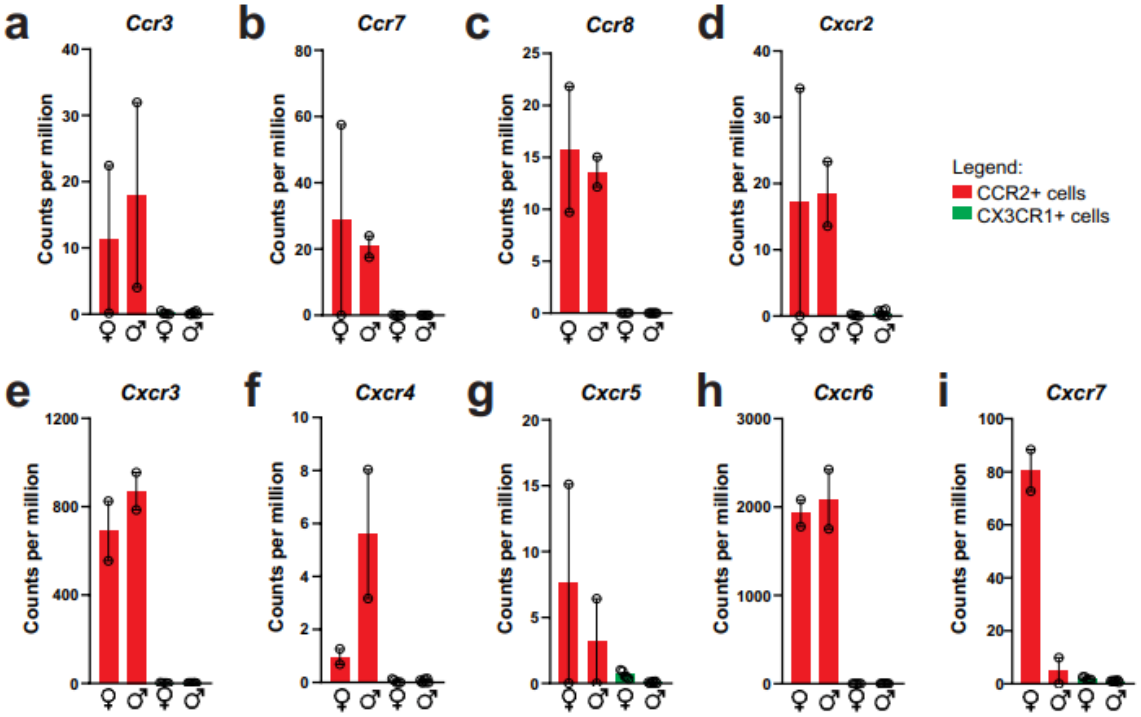

Figure 5. CCR2+ infiltrating cells from the hypothalamus of HFD-fed mice express a broad of chemokine receptors. a-i) Chemokine receptors gene expression in the transcriptome of CX3CR1+ and CCR2+ cells sorted from the hypothalamus of HFD-fed mice.

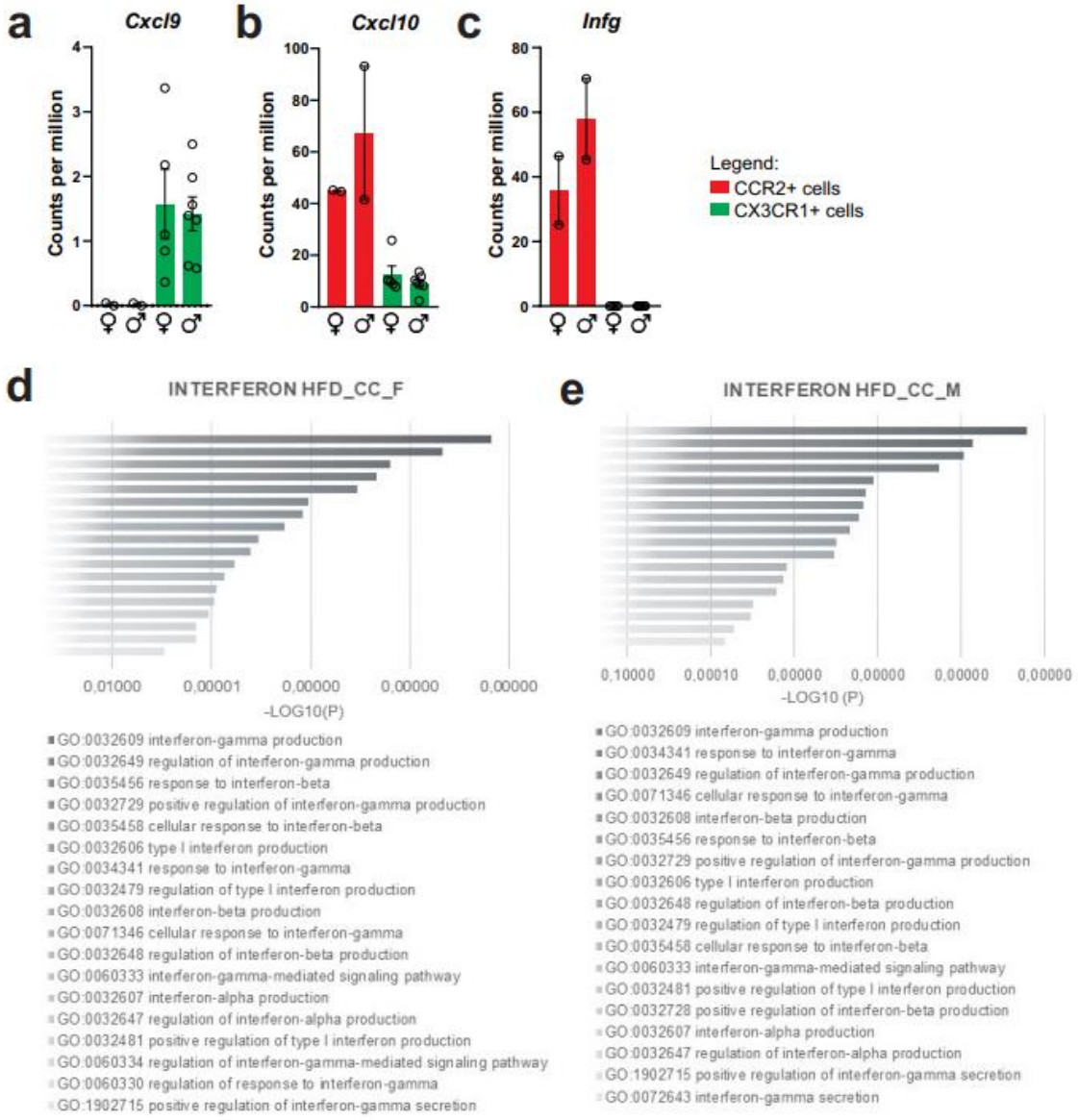

Figure 6. CXCL10/interferon γ-induced protein 10 kDa (IP-10) is highly expressed in CCR2+ infiltrating cells from the hypothalamus of HFD-fed mice. a-c) Cxcl9, Cxcl10 and Ifng gene expression in the transcriptome of CX3CR1+ and CCR2+ cells sorted from the hypothalamus of HFD-fed mice. d-e) Ontology analysis for DGEs related to interferon signaling pathways from CCR2+ cells sorted from the hypothalamus of HFD-fed female and male mice, respectively.

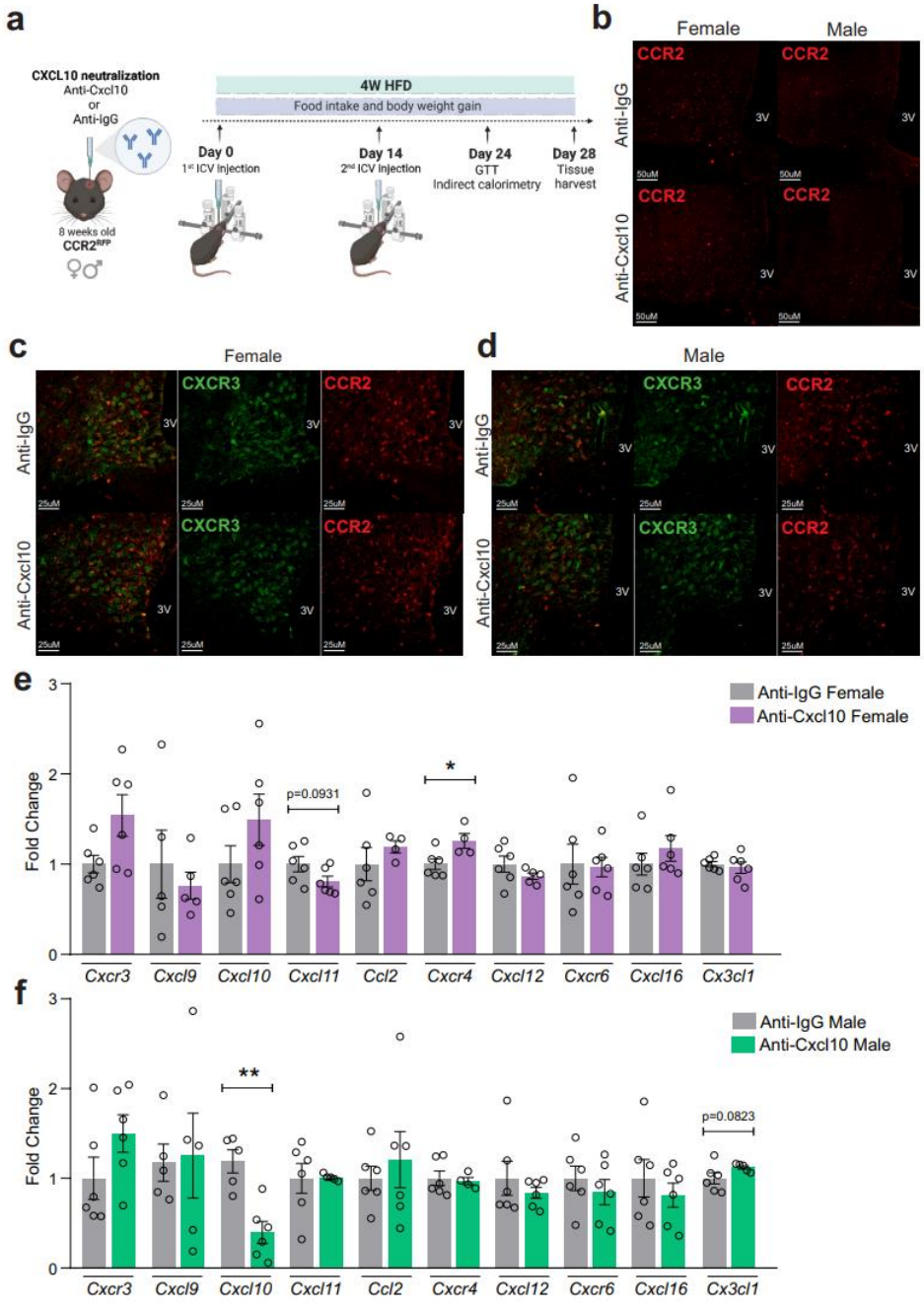

Figure 7. CXCL10 neutralization has a mild impact on reducing CCR2+ and CXCR3+ cell chemotaxis towards the hypothalamus of HFD-fed mice. a) Schematic representation of the experimental protocol for CXCL10 central neutralization. b) Coronal brain sections from 4 weeks HFD-fed CCR2^{RFP} mice showing the CCR2+ cells distribution in the hypothalamic parenchyma upon CXCL10 central neutralization. 3V = Third ventricle, Scale Bars = 50 µm. c) Coronal brain sections from 4 weeks HFD-fed female CCR2^{RFP} mice immunostained for CXCR3 upon CXCL10 central neutralization. d) Coronal brain sections from 4 weeks HFD-fed male CCR2^{RFP} mice immunostained for CXCR3 upon CXCL10 central neutralization. 3V = Third ventricle, Scale Bars = 25 µm. e-f) Hypothalamic mRNA levels of several chemokine receptors and chemokines in HFD-fed female (light gray and purple bars) and male (light gray and green bars) CCR2^{RFP} mice upon CXCL10 central neutralization. For qualitative confocal image analysis, we have used 3 samples per group. For RT-qPCR of hypothalamus we have used 5-6 samples per group. Two-tailed Mann-Whitney tests were used for statistical analyses. *p<0.05 and **p<0.01 in comparison with respective Anti-IgG treated groups.

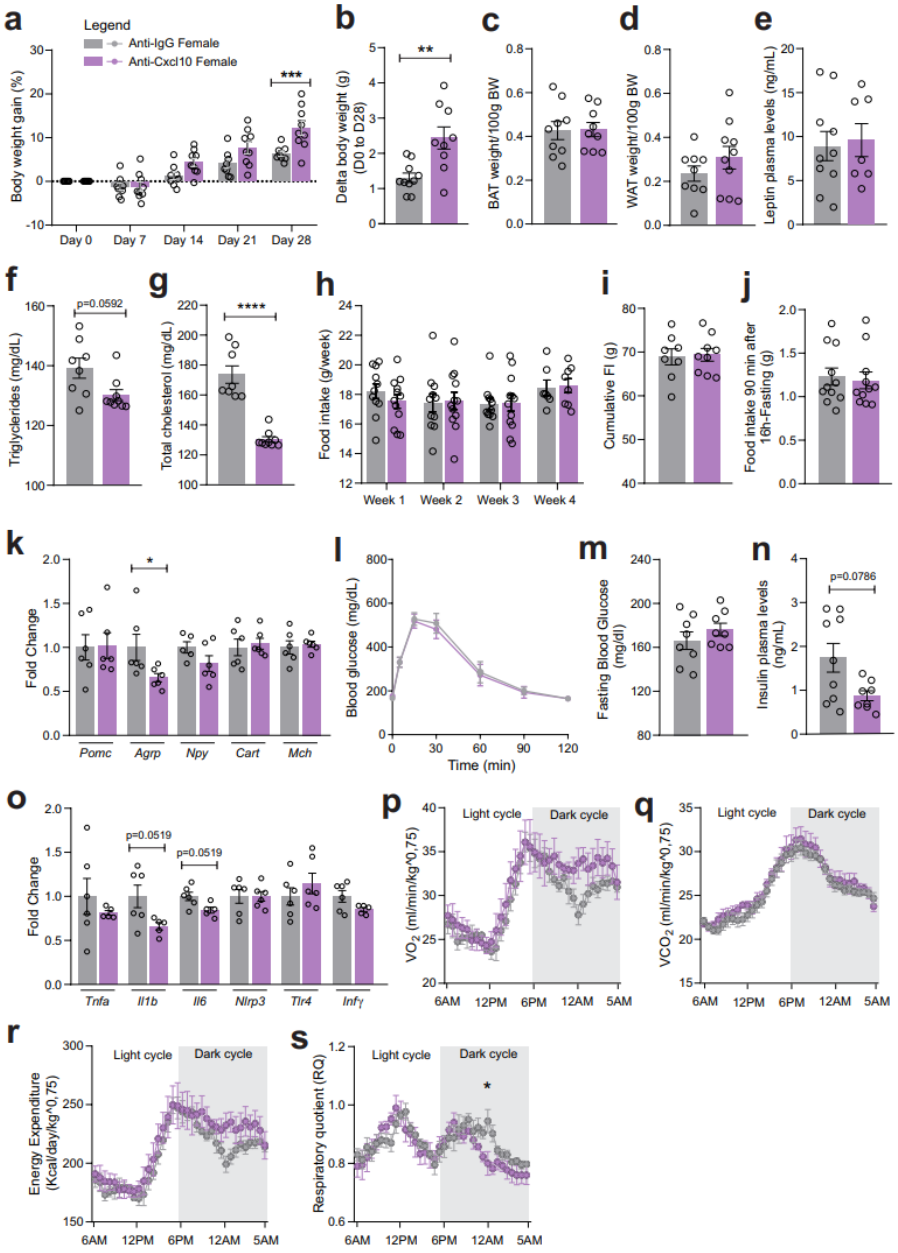

Figure 8. CXCL10 central neutralization in HFD-fed female mice. a) Percentual of body weight gain from Day 0 to Day 28 of the experimental protocol. b) Delta body weight during the experimental period. c) Brown adipose tissue weight and d) White adipose tissue (retroperitoneal depot) weight at Day 28. e) Leptin, f) Triglycerides and g) Total cholesterol plasma levels at Day 28. h) Weekly food intake measurement during experimental period. i) Cumulative food intake during the experimental period. j) 90 min food intake measurement after 16h-fasting. k) Hypothalamic mRNA levels of neuropeptides involved in food intake control. l) Intraperitoneal glucose tolerance test at Day 24. m) 6h-fasting blood glucose levels. n) Insulin plasma levels at Day 28. o) Hypothalamic mRNA levels of inflammatory genes. p) O_2 consumption; q) CO_2 production; r) Energy Expenditure and s) Respiratory Quotient at Day 24. Data were expressed as mean ± SEM of 8-10 mice per group (in two independent experiments). To perform qRT-PCR we have used 6 mice/group. To perform biochemical analysis in plasma we have used 8-10 mice/group. To perform ipGTT we have used 4 mice/group. To perform indirect calorimetry, we have used 4 mice/group. Two-way ANOVA following by Sidak's post-hoc test and Mann-Whitney test were used for statistical analyses. *p<0.05, **p<001, ***p<0.001, ****p<0.0001 in comparison with IgG treated group.

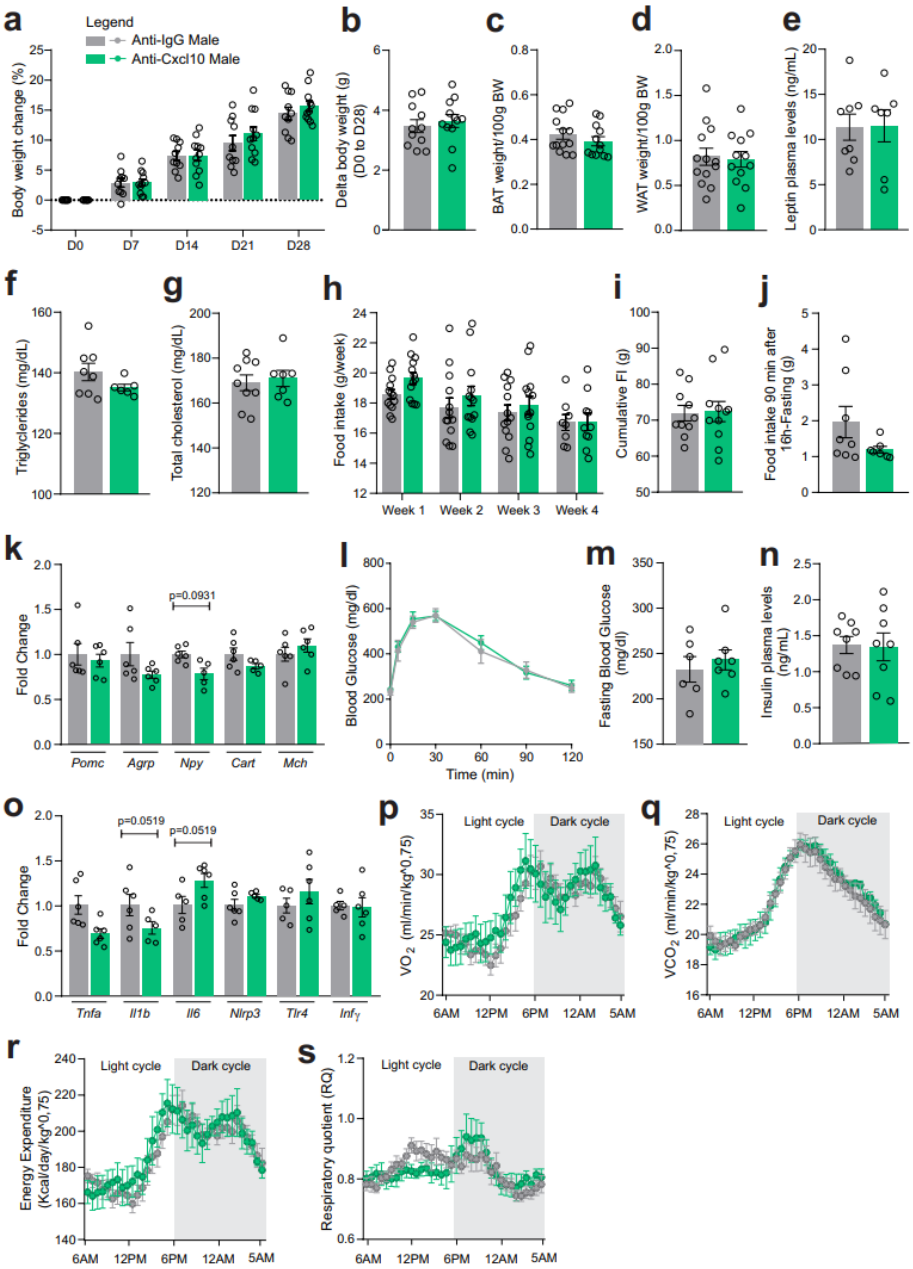

Figure 9. CXCL10 central neutralization in HFD-fed male mice. a) Percentual of body weight gain from Day 0 to Day 28 of the experimental protocol. b) Delta body weight during the experimental period. c) Brown adipose tissue weight and d) White adipose tissue (retroperitoneal depot) weight at Day 28. e) Leptin, f) Triglycerides and g) Total cholesterol plasma levels at Day 28. h) Weekly food intake measurement during experimental period. i) Cumulative food intake during the experimental period. j) 90 min food intake measurement after 16h-fasting. k) Hypothalamic mRNA levels of neuropeptides involved in food intake control. l) Intraperitoneal glucose tolerance test at Day 24. m) 6h-fasting blood glucose levels. n) Insulin plasma levels at Day 28. o) Hypothalamic mRNA levels of inflammatory genes. p) O_2 consumption; q) CO_2 production; r) Energy Expenditure and s) Respiratory Quotient at Day 24. Data were expressed as mean ± SEM of 8-10 mice per group (in two independent experiments). To perform qRT-PCR we have used 6 mice/group. To perform biochemical analysis in plasma we have used 8-10 mice/group. To perform ipGTT we have used 4 mice/group. To perform indirect calorimetry, we have used 4 mice/group. Two-way ANOVA following by Sidak's post-hoc test and Mann-Whitney test were used for statistical analyses. *p<0.05, **p<001, ***p<0.001, ****p<0.0001 in comparison with IgG treated group.

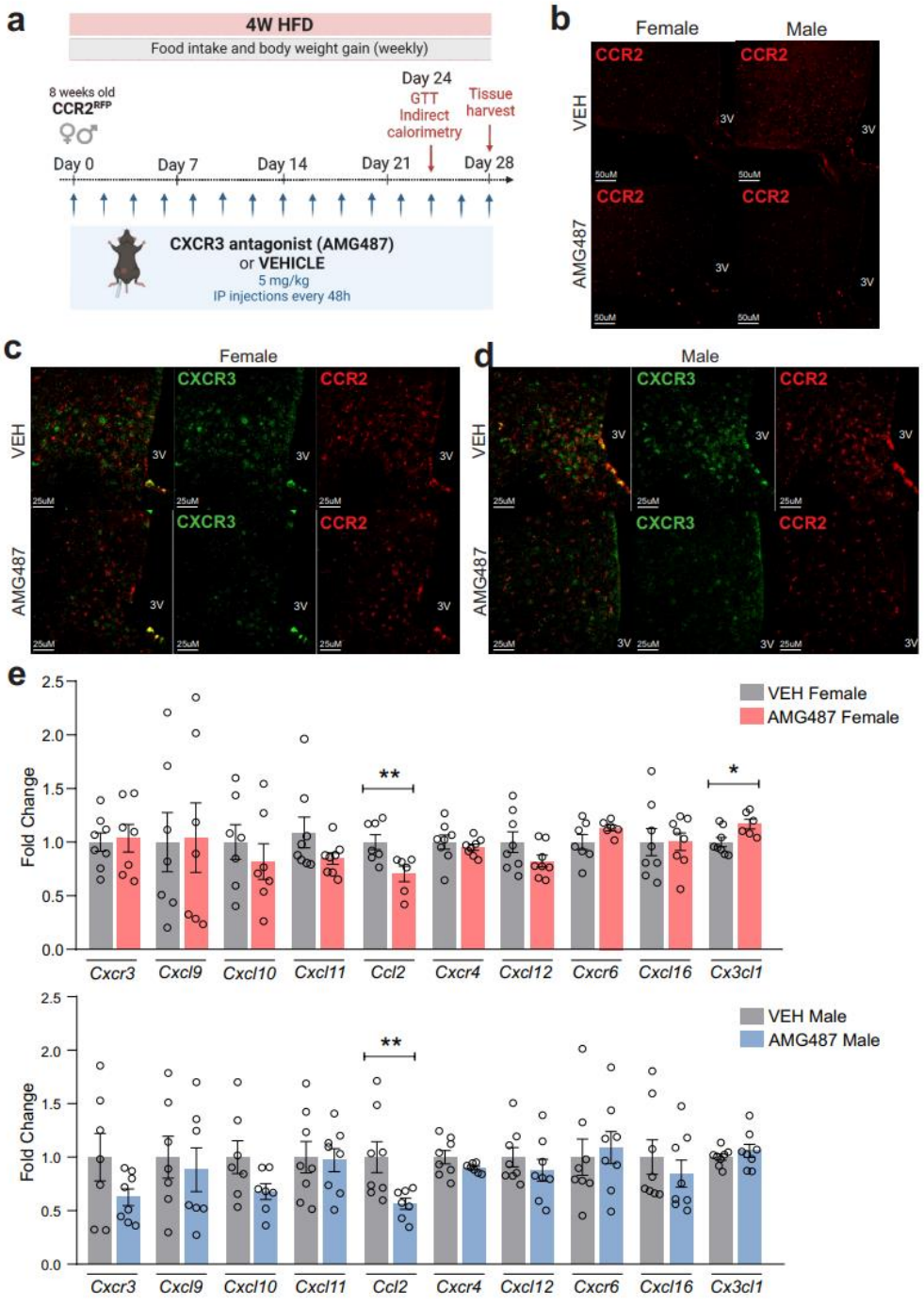

Figure 10. AMG487 treatment attenuates CCR2+ and CXCR3+ cell chemotaxis towards the hypothalamus of HFD-fed mice. a) Schematic representation of the experimental protocol for CXCR3 systemic blockage. b) Coronal brain sections from 4 weeks HFD-fed CCR2^{RFP} mice showing the CCR2+ cells distribution in the hypothalamic parenchyma upon AMG487 treatment. 3V = Third ventricle, Scale Bars = 50 µm. c) Coronal brain sections from 4 weeks HFD-fed female CCR2^{RFP} mice immunostained for CXCR3 upon AMG487 treatment. d) Coronal brain sections from 4 weeks HFD-fed male CCR2^{RFP} mice immunostained for CXCR3 upon AMG487 treatment. 3V = Third ventricle, Scale Bars = 25 µm. e-f) Hypothalamic mRNA levels of several chemokine receptors and chemokines in HFD-fed female (light gray and pink bars) and male (light gray and blue bars) CCR2^{RFP} mice upon AMG487 treatment. For qualitative confocal image analysis, we have used 3 samples per group. For RT-qPCR of hypothalamus we have used 7-8 samples per group. Two-tailed Mann-Whitney tests were used for statistical analyses. *p<0.05 and **p<0.01 in comparison with respective VEH treated groups.

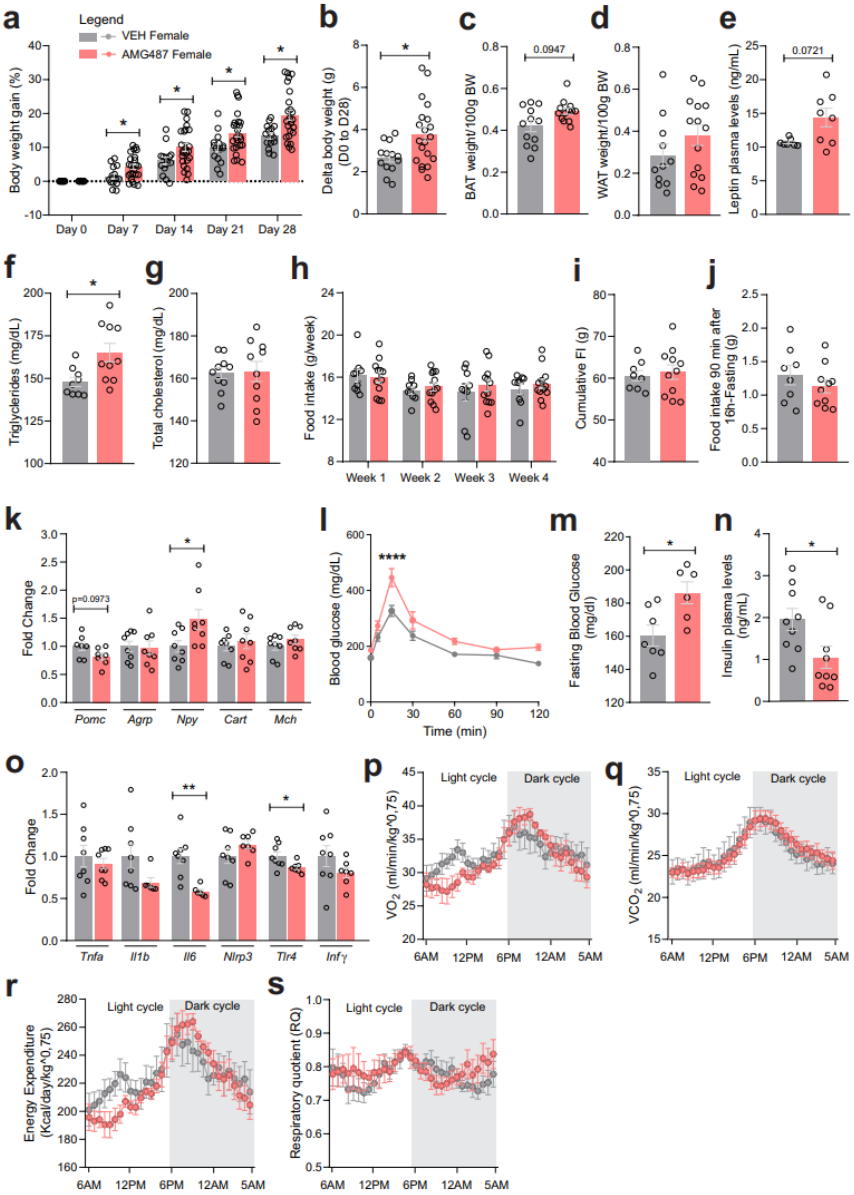

Figure 11. CXCR3 systemic blockage in HFD-fed female mice. a) Percentual of body weight gain from Day 0 to Day 28 of the experimental protocol. b) Delta body weight during the experimental period. c) Brown adipose tissue weight and d) White adipose tissue (retroperitoneal depot) weight at Day 28. e) Leptin, f) Triglycerides and g) Total cholesterol plasma levels at Day 28. h) Weekly food intake measurement during experimental period. i) Cumulative food intake during the experimental period. j) 90 min food intake measurement after 16h-fasting. k) Hypothalamic mRNA levels of neuropeptides involved in food intake control. l) Intraperitoneal glucose tolerance test at Day 24. m) 6h-fasting blood glucose levels. n) Insulin plasma levels at Day 28. o) Hypothalamic mRNA levels of inflammatory genes. p) O2 consumption; q) CO2 production; r) Energy Expenditure and s) Respiratory Quotient at Day 24. Data were expressed as mean ± SEM of 14-16 mice per group (in four independent experiments). To perform qRT-PCR we have used 8 mice/group. To perform biochemical analysis in plasma we have used 8-10 mice/group. To perform ipGTT we have used 5 mice/group. To perform indirect calorimetry, we have used 4-5 mice/group. Two-way ANOVA following by Sidak's post-hoc test and Mann-Whitney test were used for statistical analyses. *p<0.05, **p<001, ***p<0.001, ****p<0.0001 in comparison with VEH treated group.

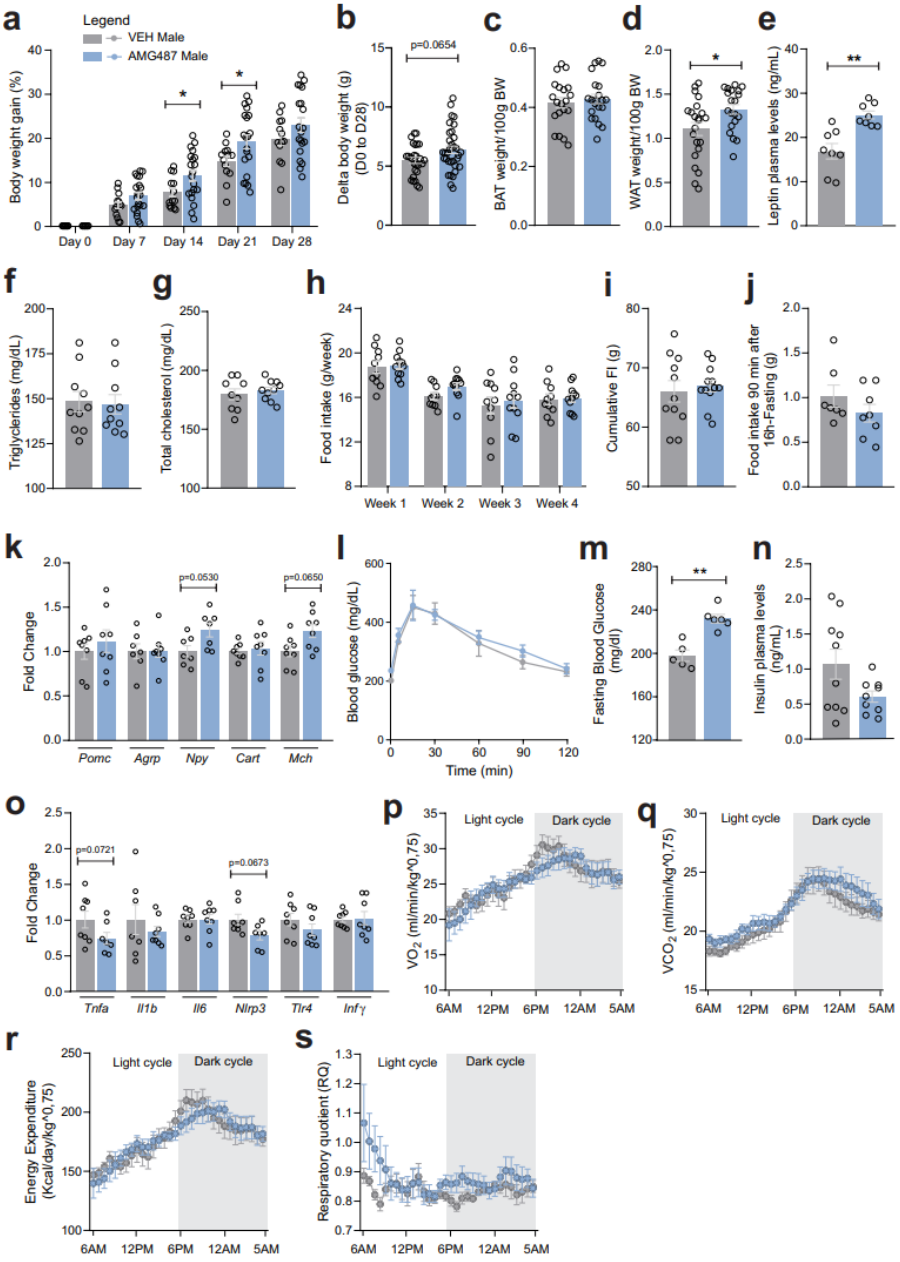

Figure 12. CXCR3 systemic blockage in HFD-fed male mice. a) Percentual of body weight gain from Day 0 to Day 28 of the experimental protocol. b) Delta body weight during the experimental period. c) Brown adipose tissue weight and d) White adipose tissue (retroperitoneal depot) weight at Day 28. e) Leptin, f) Triglycerides and g) Total cholesterol plasma levels at Day 28. h) Weekly food intake measurement during experimental period. i) Cumulative food intake during the experimental period. j) 90 min food intake measurement after 16h-fasting. k) Hypothalamic mRNA levels of neuropeptides involved in food intake control. l) Intraperitoneal glucose tolerance test at Day 24. m) 6h-fasting blood glucose levels. n) Insulin plasma levels at Day 28. o) Hypothalamic mRNA levels of inflammatory genes. p) O2 consumption; q) CO2 production; r) Energy Expenditure and s) Respiratory Quotient at Day 24. Data were expressed as mean ± SEM of 14-16 mice per group (in four independent experiments). To perform qRT-PCR we have used 8 mice/group. To perform biochemical analysis in plasma we have used 8-10 mice/group. To perform ipGTT we have used 5 mice/group. To perform indirect calorimetry, we have used 4-5 mice/group. Two-way ANOVA following by Sidak's post-hoc test and Mann-Whitney test were used for statistical analyses. *p<0.05, **p<001, ***p<0.001, ****p<0.0001 in comparison with VEH treated group